END

MICROCOPY RESOLUTION TEST CHART

NATIONAL BUREAU OF STANDARDS-1963-A

AD-A163 826

DTIC
S **ELECTE**
FEB11
D
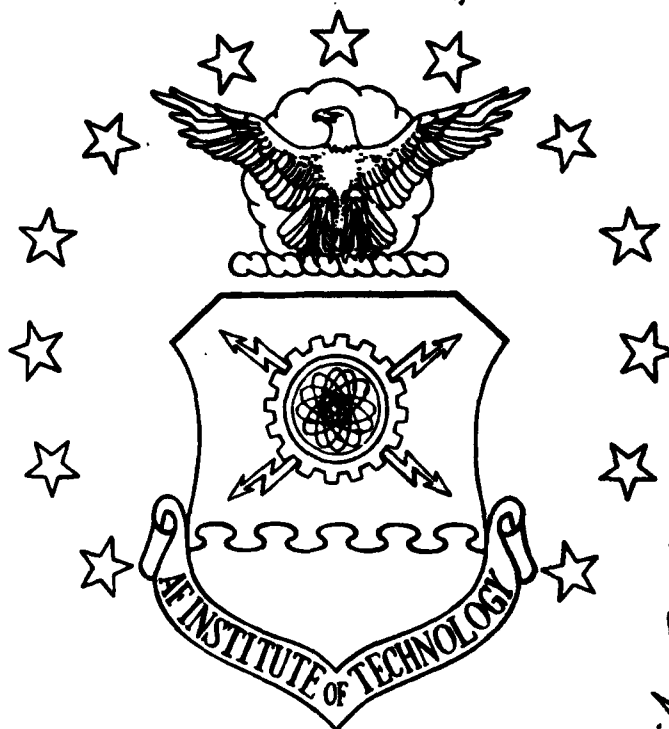
DISTRIBUTION FILE COPY

PHYSICAL OPTICS MODEL OF
SIDE LOBE NULLING BY DISCS
ON A PARABOLIC REFLECTOR

THESIS

Dick A. Trapp
Captain, USAF

AFIT/GE/ENG/85-51

DEPARTMENT OF THE AIR FORCE

AIR UNIVERSITY

AIR FORCE INSTITUTE OF TECHNOLOGY

Wright-Patterson Air Force Base, Ohio

86 2 10 024

DTIC

S **ELECTE**

FEB 1 1 1986

D

D

PHYSICAL OPTICS MODEL OF
SIDE LOBE NULLING BY DISCS
ON A PARABOLIC REFLECTOR

THESIS

Dick A. Trapp
Captain, USAF

AFIT/GE/ENG/85-51

AFIT/GE/ENG/85D-51

PHYSICAL OPTICS MODEL OF

SIDE LOBE NULLING BY DISCS

ON A PARABOLIC REFLECTOR

THESIS

Presented to the Faculty of the School of Engineering

of the Air Force Institute of Technology

Air University

In Partial Fulfillment of the

Requirements for the Degree of

Master of Science in Electrical Engineering

Dick A. Trapp, B.S.

Captain, USAF

December 1985

Approved for public release; distribution unlimited

Accesion For	
NTIS CRA&I	☑
DTIC TAB	☐
Unannounced	☐
Justification	
By	
Distribution /	
Availability Codes	
Dist	Avail and / or Special
A-1	

i

Acknowledgments

Table of Contents

List of Figures

Abstract

By mounting small disc reflectors that are moveable relative to the inner reflector surface of a parabolic dish antenna, nulls can be generated in the side lobe region of the power radiation pattern with minimal distortion effects to the main beam. A physical optics model of this antenna system is developed to investigate in a simplified direct manner the phenomena of phase nulling caused by disc movement.

Array theory using isotropic radiators is used to sample the aperture distribution to approximate the far field electric field of the dish. A physical optics approximation for scattering off a flat metal disc is used for discs and feed blockage effects. The array theory term plus the feed blockage term yields the field intensity quiescent patterns, phase and amplitude, proportional to $|\bar{E}_{Quiescent}(\theta,\phi)|$. The physical optics term for the discs yields the field intensity cancellation patterns, phase and amplitude, proportional to $|\bar{E}_{Cancellation}(\theta,\phi)|$. The quiescent patterns are combined with the cancellation patterns to produce the relative power pattern, nulled pattern, proportional to $|\bar{E}_{Total}(\theta,\phi)|^2$. No secondary effects such as diffraction or edge illumination are considered.

A computer code was written to implement this approach and the theoretical patterns produced. Actual measured patterns are compared to the theoretical patterns. There is good agreement between theory and actual measurements. Finally applications of this antenna system are presented.

PHYSICAL OPTICS MODEL OF SIDE LOBE NULLING BY DISCS ON A PARABOLIC REFLECTOR

I. Introduction

Background

Dr. J. Leon Poirier and Daniel Jacavanco at the Electromagnetic Sciences Division, Rome Air Development Center, first proposed the idea of adaptive nulling by Electrostatically Controlled Membrane Reflectors (EMR) such as Figure 1.
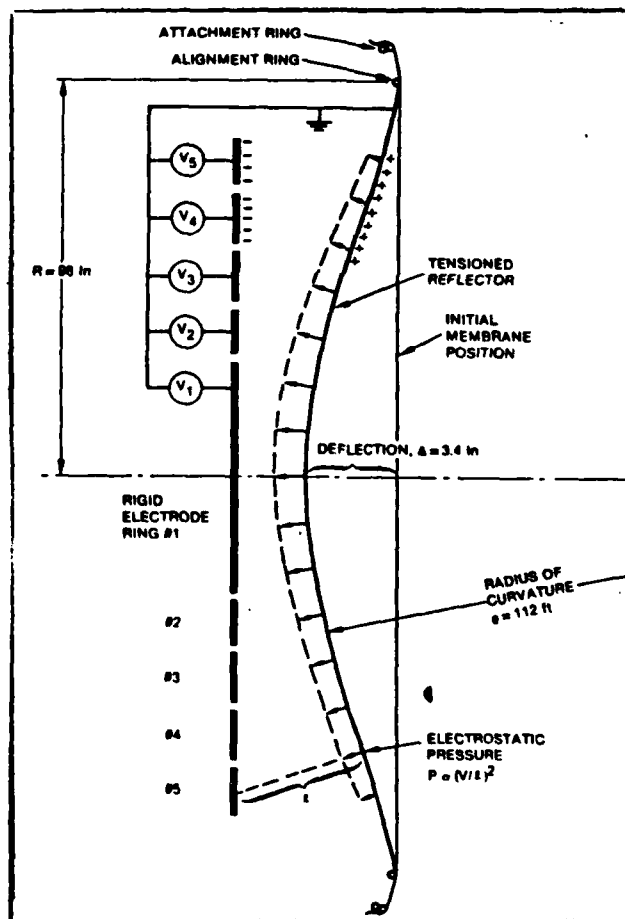
Figure 1. Electrostatic Membrane Reflector (Adaptive Reflector, 1984c)

This type of reflector antenna was originally proposed for space applications (Lang, 1978). The feedback circuitry of (EMR) could be used to systematically distort the reflector surface to form nulls in selected directions of the side lobe region of the antenna. A distortion of the reflector surface would change the phase of a corresponding region of the aperture field distribution thus generating a perturbation in the radiation pattern. By appropriate control of the feedback circuitry a null could be "moved" in the desired direction to eliminate any interference from that direction. The theoretical basis for this scheme was investigated by Havens (Havens, 1983). It was found that the control problem of maintaining a perfect shape, such as a paraboloid was extremely difficult. Thus, the use of selective distortion appeared too complicated for practical use.

Historically adaptive nulling in the side lobe region has been accomplished by arrays. Computer controlled, these antennas are capable of steering their main beams and nulls. Array antennas, however, are complex, costly, and heavy in comparison with reflector antennas.

"In the summer of 1983 Jacavanco demonstrated it was possible to produce nulls in the pattern of a rigid reflector by mounting discs on the reflector dish and adjusting their distance off the dish by computer algorithm controlled motors as shown in Figure 2" (Rudisill, 1984b:1).
These antennas are much simpler to construct and offer high maximum gain per unit weight. This approach offers flexibility

2

and improved signal to noise ratios in an already widely used
antenna. Indeed this has been proven for a multitude of
parabolic reflectors, multiple disc sizes, and disc placement by
Jacavanco at the Electromagnetic Sciences Division since the
summer of 1983.
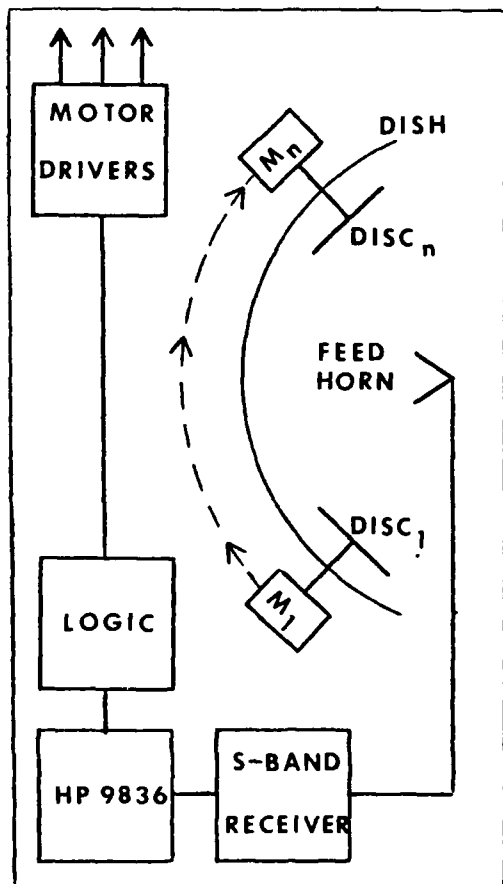
Figure 2. Computer Controlled Discs---Parabolic Reflector
(Adaptive Reflectors, 1984c; Research, 1985bc)

From January to November 1984, Rudisill developed a
theoretical background for the system of Figure 2. He used
aperture integration and modeled the disc's effect on

3

the aperture field as a phase shift across a circular projection of the disc into the aperture plane. The feed was assumed to produce a parabolically tapered electric field. This approach required large amounts of computer time for numerical integration and theoretical results from the model compared poorly to experimental results. He concluded this to be a result of too idealistic an antenna model rather than error in basic theory (Rudisill, 1984a:7,59).

During this same period Jacavanco modeled the system of Figure 2 using linear array theory. His model showed with reasonable accuracy the salient features of nulling with two discs (Jacavanco, 1984b).

Approach

The present approach is similar to Jacavanco's linear array model. It uses 841 isotropic radiators spaced 0.25 wavelengths apart to simulate the actual normalized aperture distribution, approximating the far zone electric field of the reflector. The disc and feed blockage effects are approximated using a physical optics method of scattering by flat metal discs, assumed to be perfectly conductive (see Figure 3). All three terms are combined to produce a system relative power pattern in the H-plane. The Relative Power Pattern is proportional to

$$|\overline{E}_{TOT}(\theta,\phi=0)|^2 = |\overline{E}_D(\theta,\phi=0)+\overline{E}_{S12}(\theta,\phi=0)-\overline{E}_{FB}(\theta,\phi=0)|^2 \qquad (1\text{-}1)$$

(Total) (Dish) (Scattering (Feed
Discs 1&2) Blockage)

4

where: $\overline{\overline{\mathbf{E}}}_{TOT}(\theta,\phi=0)$ is the total complex vector electric field for the H-plane.

$\overline{\overline{\mathbf{E}}}_{D}(\theta,\phi=0)$ is the total complex vector electric field from the reflector without discs and feed blockage.

$\overline{\mathbf{E}}_{S12}(\theta,\phi=0)$ is the complex vector electric field from scattering off the two discs.

$\overline{\overline{\mathbf{E}}}_{FB}(\theta,\phi=0)$ is the complex vector electric field from scattering off the parasitic reflector.
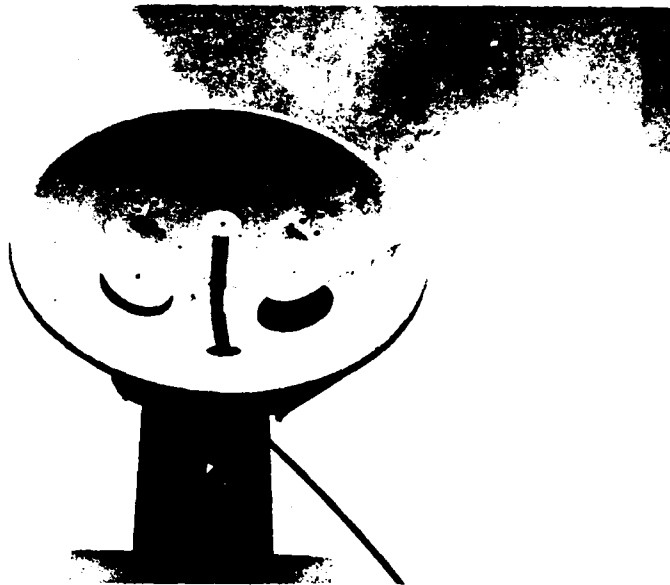
Figure 3.   Two Discs on a Parabolic Reflector

"The effect of the aperture blocking can be approximated by subtracting the radiation pattern produced by the obstacle from the radiation pattern of the undisturbed aperture" (Skolnick, 1962:269). A description of the system follows this section.

5

Antenna System Description

The antenna system modeled is shown again in Figure 4 for reference. The drive motors are not attached in Figure 4.
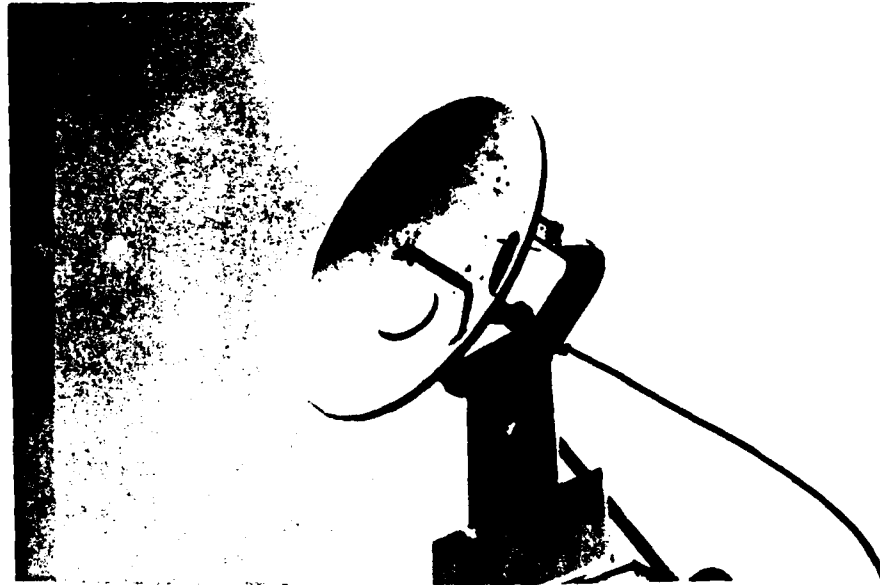
Figure 4.   Antenna System Modeled
(Research, 1985bc)

The antenna is a prime-focus, S-band, general purpose, parabolic reflector. It was driven at 3.12 Ghz through a rear fed half-wave dipole using a parasitic circular reflector disc at a distance equal to one-fourth wavelength from the dipole. The dish measures two feet in diameter and the focal distance from dish vertex to parasitic reflector is 6.8 inches. The feed polarization is assumed to be purely linear in the vertical (-y) direction (see Coordinate System page 14). The feed blockage is assumed to be a two inch diameter disc at the center of the aperture plane. The discs are five inches in diameter and are placed symmetrically six inches from the feed arm. The

supporting rods that move them, relative to the reflector inner
surface, lie on a common line with the dish vertex and
perpendicular to the dipole direction (see Figure 5).
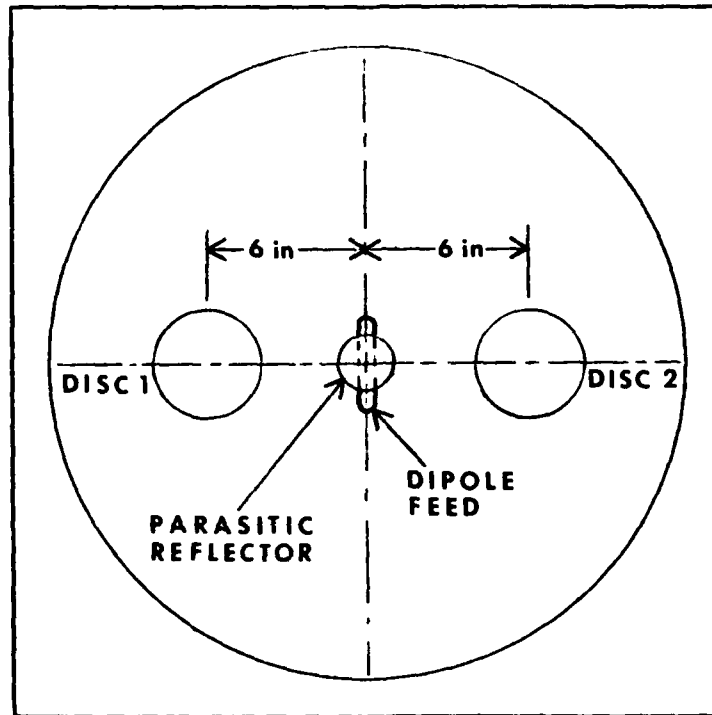
Figure 5. Disc Location: Front View (Not to Scale)

Generating a Nulled Relative Power Pattern

The antenna system is mounted on a pedestal that can move in
azimuth or elevation planes (see Figure 6). A pyramidal horn,
175 feet away acts as a transmitter/jammer. The transmitter
illuminates the frontal aspect of the dish at 3.12 Ghz and is
assumed to be in the far field of the antenna. It is assumed

Figure 6. Antenna Mounted on Pedestal
(Research, 1985bc)

plane waves of one milliwatt intensity, vertically polarized are

intercepted by the dish. The pedestal is fixed in the elevation

plane so that only azimuthal rotation occurs. Since the

incident E-field is vertically polarized, this rotation will

generate on H-plane pattern. The discs are held flush on the

inner reflector surface (see Figure 6) and a system quiescent

power pattern is recorded. A Scientific-Atlanta Series 1580

Pattern Recorder was used. Once the quiescent pattern is

recorded it is rewound so the nulled pattern can be recorded

over it in a different color ink for comparison purposes. To

accomplish the nulled pattern the antenna is rotated so the

signal is received at some arbitrary point in the side lobe

8

region. It is held there while the system computer finds the optimum position for the discs to minimize the received signal. With the discs in the optimum position a new power pattern (nulled pattern) is recorded over the quiescent power pattern.

The antenna system uses an algorithm to minimize the received signal. It varies the discs, one at a time, from flush to their maximum out extension (1/2 Revolution = 1/32 inch out from reflector surface) through thirty-two possible positions. At each position the actual distances of the discs from the reflector surface are recorded as electric phase angles and the Power Total (PTOT) is recorded corresponding to the electric phase angles. A gradient search of the data is performed for the combination of phase angles and PTOT that yields the minimum PTOT. The computer then positions the discs via their motors to the optimum position.

The next chapter will discuss the theory involved with the nulling phenomena caused by disc movement.

II. Theory

Phase Nulling With Discs

The tactical situation this system could be used in is this:
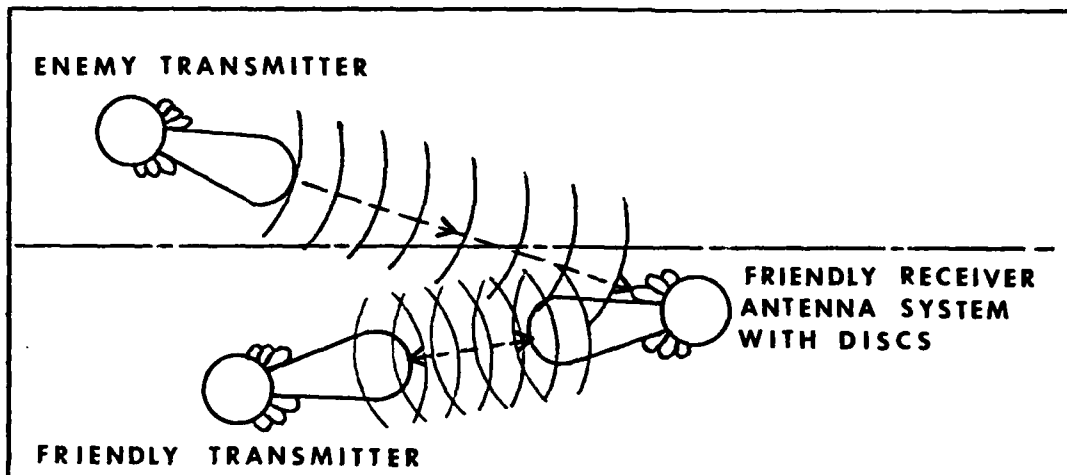
Figure 7.   Tactical Situation for System Use

The enemy transmitter is jamming us through the receiver
antenna's side lobes. The receiver antenna's power pattern by
reciprocity is the same as its power pattern when it transmits.
If a null can be shifted in the receiver antenna power pattern,
in the jammer transmitter direction, we can negate the jamming
interference. If the jamming interference can be split into two
electric field components of the same amplitude but with phases
180° opposite, they will cancel each other completely due to
the destructive interference of two coherent signals, equation
(2-1), (two sinusoids at the same frequency) (Research,1985b).
Refer to equation (2-1) and Figure 8 on the next page.

$$P_{TOT} = P_1 + P_2 + 2\sqrt{P_1 P_2}\cos\theta \qquad (2-1)$$

where: $P_1 = \sqrt{P_{RJQ}}$ = Amplitude of P_{RJQ}

P_{RJQ} = Power received from jammer thru dish

$P_2 = \sqrt{P_{RJD}}$ = Amplitude of P_{RJD}

P_{RJD} = Power received from jammer thru discs

θ = Phase difference angle between P_{RJQ} and P_{RJD}
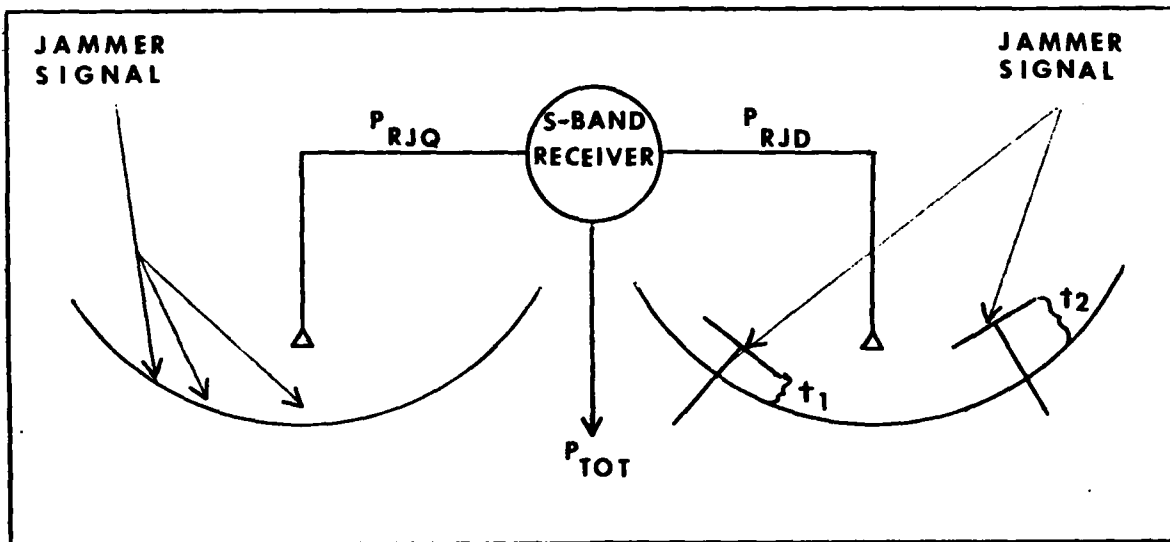
Figure 8. Nulling With Discs

Therefore by choosing the correct size and disc location and adjusting t_1 and t_2 (see Figure 8) until

$$\sqrt{P_{RJQ}}e^{j\phi_1} + \sqrt{P_{RJD}}e^{j\phi_2} \approx 0 \qquad (2-2)$$

then the antenna system will move a null in the side lobe region of the power radiation pattern in the direction of the

11

interfering source. The correct size and disc location has been determined by Jacavanco (Jacavanco, 1984b:1,2). "If nulling is desired in a uniformly illuminated reflector in the region of the pattern where the response is down 30dB from the main beam peak, then the total area of the reflector minus the total area of the two discs should also be down by 30dB. In an antenna in which the feed horn imposes a tapered illumination across the dish for side lobe control, the size and position of the discs should be further modified. For the same performance, a larger disc is required if positioned in the region of lower intensity than a disc positioned in a region of higher intensity (near the center)." Another factor is that disc size and placement on the reflector surface should not degrade the main beam. This has been experimentally proven by Jacavanco (Jacavanco, 1984ab). A simplified picture of the entire system is presented in Figure 9 (only one disc shown for clarity).

where: P_{RSQ} = Power received from signal thru dish

P_{RSD} = Power received from signal thru discs

P_{RJQ} = Power received from jammer thru dish

P_{RJD} = Power received from jammer thru discs
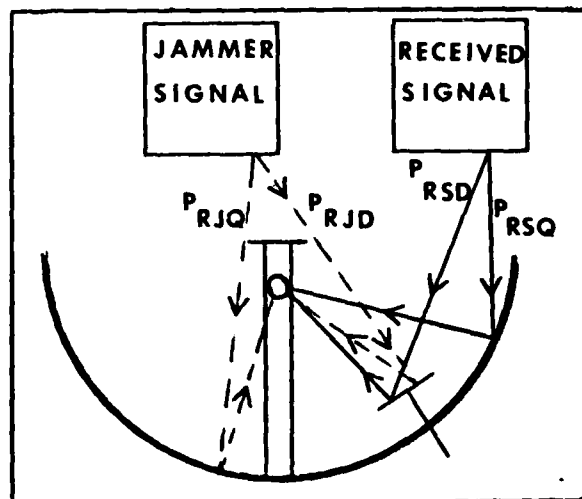
Figure 9. Simplified System

12

So the Total Power received is

$$P_{TOT} = P_{RSQ} + P_{RSD} + P_{RJQ} + P_{RJD} \qquad (2-3)$$

Therefore the discs are moved to minimize P_{TOT} by phase cancellation between P_{RJQ} and P_{RJD}. Since $P_{RSQ} \gg P_{RSD}$ the signal received will be P_{RSQ}, the desired signal.

System Coordinate Reference

The reference system used with the isotropic radiators in the aperture plane (xy plane at z = q) is shown on the next page in Figure 10. The z = 0 phase reference is at the actual pivot point for the antenna system mounted on the pedestal (see Figure 6). Where they are more convenient, spherical coordinates are used and coordinates that refer to the aperture plane (source) will be primed any time there is any confusion. Far field patterns are presented in rectangular coordinates. Complex scalars are designated by underbars and complex vectors are designated by both overbars and underbars. Unit vectors are designated by "hats", in other words, $\hat{x}$ is the unit vector in the x-direction.

−Y

etc col +2 col +1 col 0 col −1 col −2 etc

(+) ◄─────── (m) ───────► (−)

PHASE
Z=0: REFERENCE

+X ◄─────────────────────────────────

(−)

etc
row 2
row 1
row 0 (n) ◄───
row 1
row 2
etc

(+)

+Z

interelement
spacing: $l = \dfrac{\lambda}{4}$

n

w: (ave distance
to disc
flush position)

+Y

q: (distance to
array in
aperture
plane)
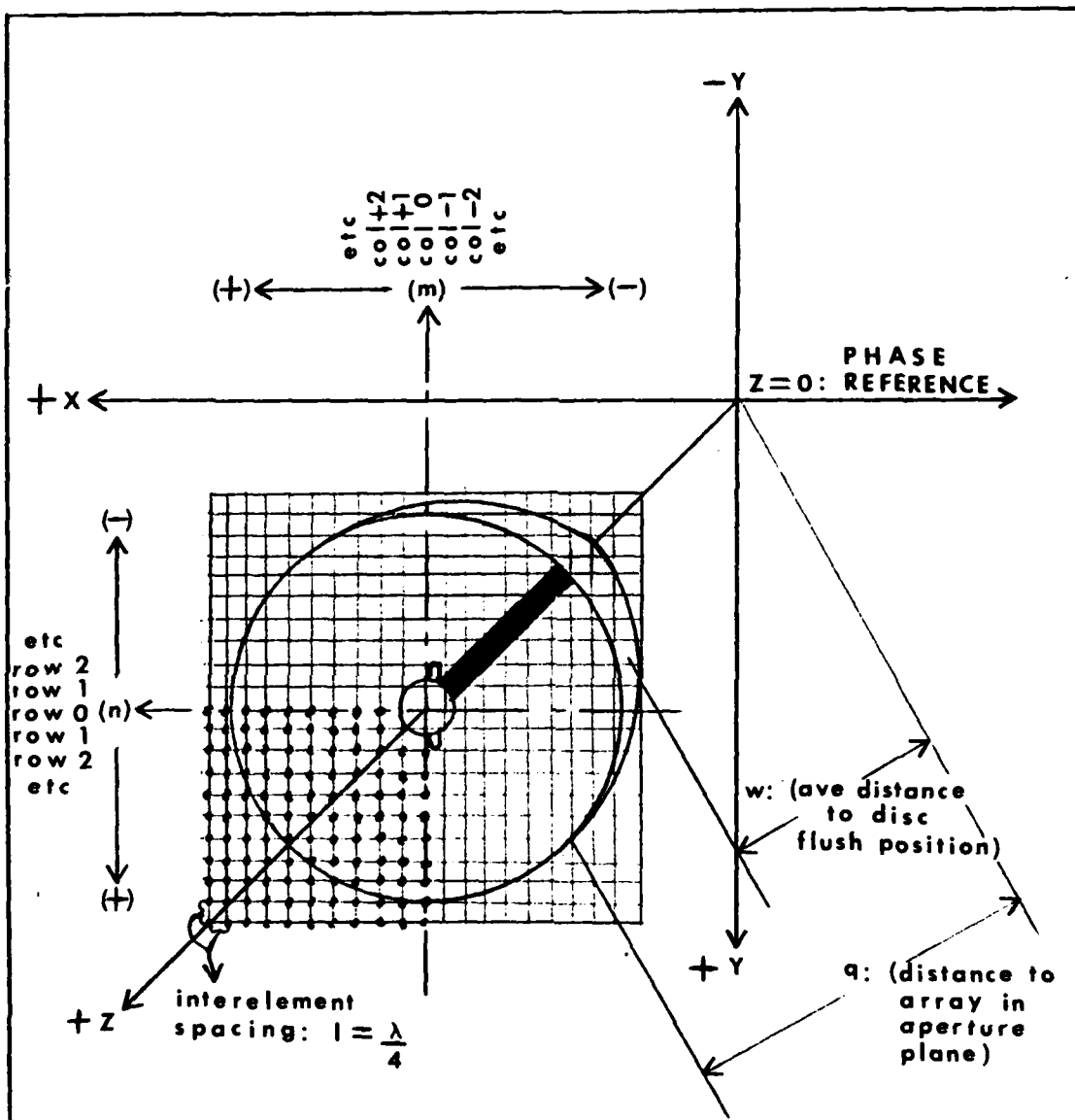
Figure 10. System Coordinate Reference

14

Array Theory: E-field of the Reflector Only

To restate the problem: How does the phase of the electric fields from the discs interact with the phase of the electric fields in the side lobe region of the dish? This causes cancellation, which ultimately perturbs the power radiation pattern; shifting side lobe nulls to new angles. Reviewing the approach from Eq (1-1)

$$|\overline{E}_{TOT}(\theta,\phi=0)|^2 = |\overline{E}_D(\theta,\phi=0)+\overline{E}_{S12}(\theta,\phi=0)-\overline{E}_{FB}(\theta,\phi=0)|^2$$

The development of $\overline{E}_D(\theta,\phi=0)$ follows. The aperture plane currents of the dish alone will be sampled using linear array theory starting from the complex vector potential. $\overline{E}_D(\theta,\phi=0)$ will be derived from the complex vector potential. The complex vector potential is given by (Stutzman and Thiele, 1962:455):

$$\overline{A} = \iint\limits_{Source} \frac{\overline{J}\,e^{j\beta R}}{4\pi R}\,ds \tag{2-4}$$

where: $\overline{J}$ = currents in aperture plane

R = distance between source points and observation points

$\beta = \frac{2\pi}{\lambda}$

Assuming parallel rays, R for the phase is determined by geometrical techniques. R in the denominator is approximated by r, an average distance from the phase reference point ($z = 0$) to the observation point (Stutsman and Thiele, 1962:22-24).

15

Therefore the complex vector potential in the far field is

$$\overline{A}_{ff}(\overline{r}') = \underline{\Psi}(r) \iint_{\overline{r}'} \underline{\overline{J}}(\overline{r}')\, e^{j\beta \overline{r}' \cdot \hat{r}}\, d\overline{r}' \qquad (2\text{-}5)$$

where: $\underline{\Psi}(r) = \dfrac{e^{-j\beta r}}{4\pi r}$

$\overline{r}'$ = vector from phase reference point to source

r = distance from phase reference point to observation point

$$\overline{r}' \cdot \hat{r} = \underbrace{x'\beta \sin\theta\cos\phi}_{-\beta_x} + \underbrace{y'\beta \sin\theta\sin\phi}_{-\beta_y} + \underbrace{z'\beta \cos\theta}_{-\beta_z}$$

$\underline{\overline{J}}(\overline{r}') = \hat{p}I_A(x')I_B(y')I_C(z')$

$\hat{p}$ = $-\hat{y}$ the transmitter polarization

Putting this all together yields

$$\overline{A}_{ff}(\overline{r}') =$$
$$-\hat{y}\underline{\Psi}(r) \int \underbrace{I_A(x')e^{-j\beta_x x'}\, dx'}_{\underline{F}_A(\beta_x)} \int \underbrace{I_B(y')e^{-j\beta_y y'}\, dy'}_{\underline{F}_B(\beta_y)} \int \underbrace{I_C(z')e^{-j\beta_z z'}\, dz'}_{\underline{F}_C(\beta_z)} \qquad (2\text{-}6)$$

where: $\underline{F}_A(\beta_x)$ = fourier transform of $I_A(x')$

$\underline{F}_B(\beta_y)$ = fourier transform of $I_B(y')$

$\underline{F}_C(\beta_z)$ = fourier transform of $I_C(z')$

We can now further simplify Eq (2-6) for $\overline{A}_{ff}(\overline{r}')$

$$\overline{A}_{ff}(\overline{r}') = -\hat{y}\underline{\Psi}(r)\underline{F}_A(\beta_x)\underline{F}_B(\beta_y)\underline{F}_C(\beta_z) \qquad (2\text{-}7)$$

16

As an example, isolating just row 0: $m \rightarrow 14$ to -14, $n = 0$,
each isotropic source can be represented by a delta function
(see Figure 10)

$$\underset{\text{row 0}}{\underline{F}_A(\beta_x)} \quad \triangleleft\text{--}\triangleright \quad \sum_{m=14}^{-14} \underline{I}_A(x')\left[\delta(x' + ml)\right]$$

$$\underset{\text{row 0}}{\underline{F}_B(\beta_y)} \quad \triangleleft\text{--}\triangleright \quad \underline{I}_B(y')\left[\delta(y' + nl)\right]$$

$$\underset{\text{row 0}}{\underline{F}_C(\beta_z)} \quad \triangleleft\text{--}\triangleright \quad \underline{I}_C(z')\left[\delta(z' + q)\right]$$

where: l,q are defined on Figure 10

$$\underline{I}_A = I_{mnq}e^{j(m\alpha)}$$

$$\underline{I}_B = I_{mnq}e^{j(n\alpha)}$$

$$\underline{I}_C = I_{mnq}e^{j(q\alpha)}$$

I_{mnq} = amplitude of each isotropic point source
according to the normalized aperture
distribution

α = interelement progressive phase difference ($\alpha = 0$)

Combining all terms for row 0 yields

$$\overline{\underline{A}}_{ff}(\overline{r}') = -\oint \underline{\psi}(r) I_{mnq}\left[\sum_{m=14}^{-14} e^{-j\beta x(ml)}\right]\left[e^{-j\beta y(nl)}\right]\left[e^{-j\beta z(q)}\right] \quad (2\text{-}8)$$

Finally, for row 0, dropping the subscript q on I_{mnq} since it
is constant and $n = 0$

$$\overline{\underline{A}}_{ff}(\overline{r}') = -\oint \underline{\psi}(r) I_{mn}\left[\sum_{m=14}^{-14} e^{-j\beta x(ml)}\right]\left[e^{-j\beta z(q)}\right] \quad (2\text{-}9)$$

But since there are 29 rows, $n \rightarrow 14$ to -14

$$\overline{\underline{A}}_{ff}(\overline{r}') =$$
$$-\oint \underline{\psi}(r) I_{mn}\left[\sum_{m=14}^{-14} e^{-j\beta x(ml)}\right]\left[\sum_{n=14}^{-14} e^{-j\beta y(nl)}\right]\left[e^{-j\beta zq}\right] \quad (2\text{-}10)$$

17

To get $\overline{E}_D(\theta,\phi=0)$ from $\overline{A}_{ff}(\overline{r}')$ for an H-plane cut ($\phi = 0$) use

$$\overline{E}_D(\theta,\phi=0) \approx -j\omega\left[\overline{A}_{ff}(\overline{r}') - \hat{r}A_{ff}(\overline{r}')\right] \qquad (2\text{-}11)$$

The radial component of $\overline{A}_{ff}(\overline{r}')$ is disregarded

$$\overline{E}_D(\theta,\phi=0) \approx \frac{\hat{\theta}jE_O\beta e^{-j\beta r}}{2\pi r}\left(e^{-j\beta zq}\left[\sum_{m=14}^{-14}\sum_{n=14}^{-14}I_{mn}e^{-j\beta x(ml)}\right]\right) \qquad (2\text{-}12)$$

where: E_O is the initial E-field amplitude received by the dish.

see Appendix A for actual values for E_O, q, l, λ.

The next step is to derive a normalized aperture distribution from which I_{mn} can be assigned.

Normalized Aperture Distribution

The feed antenna is not isotropic. The effect of the normalized feed radiation pattern, $F_f(r')$, is related to the normalized aperture distribution by this equation (Stutzman and Thiele, 1981:428):

$$E_a(r') = F_f\left(r' = 2f\,\tan\frac{\theta'}{2}\right)\left[1 + \left(\frac{r'}{2f}\right)^2\right]^{-1} \qquad (2\text{-}13)$$

where: r', θ' are spherical coordinates of the aperture plane (see Figure 10).

f is the focal distance of the reflector (see Appendix A).

The rear fed half-wave dipole using a parasitic circular
reflector disc does not produce a circularly symmetric pattern.
But the average of the E- and H-plane pattern values can be used
in Eq (2-13) according to (Stutzman and Thiele, 1981:428). This
is shown by the dotted line in Figure 11, the normalized feed
radiation pattern at 3.12 Ghz for the rear fed half-wave dipole
using a parasitic circular reflector.

E—plane pattern value
_____

H—plane pattern value
— — — — —

ave   pattern value
• • • • • • • •
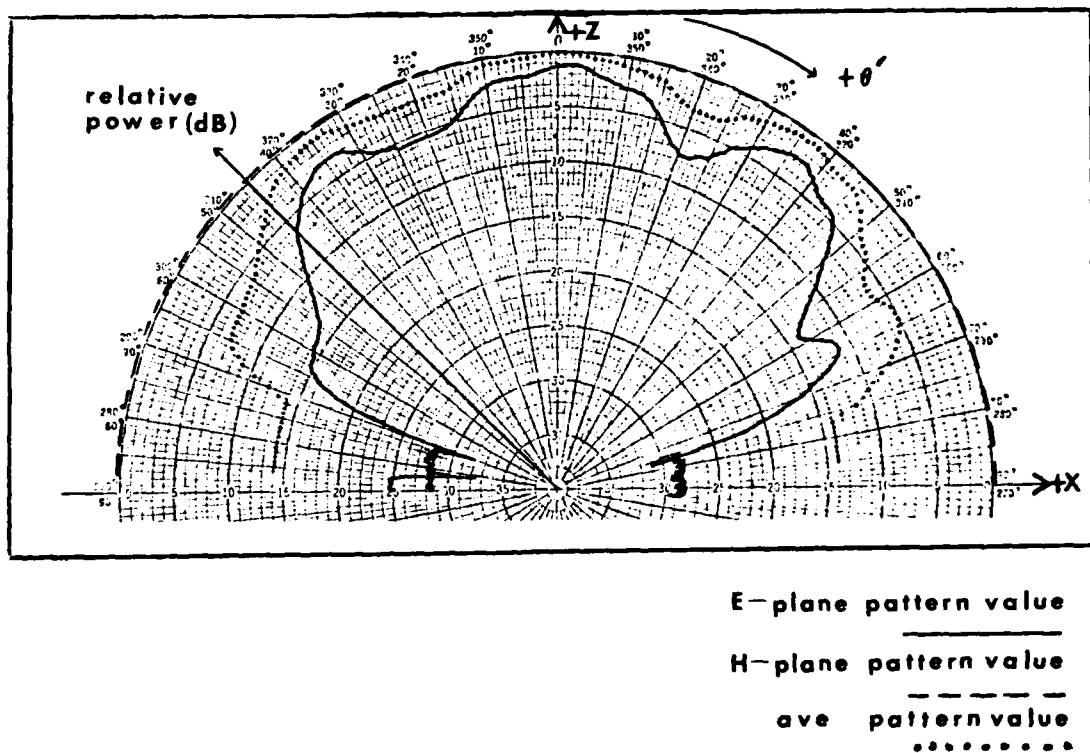
Figure 11.   Normalized Feed Radiation Pattern

To obtain $E_a(r')$, the normalized aperture distribution, r' was calculated in increments of $\theta' = 1^{\circ}$ using Eq (2-13). $F_f(r')$ was read off Figure 11, then Eq (2-13) used again to produce a plot of $E_a(r')$ (see Figure 12 next page). Finally Figure 12 was used in conjunction with a scale drawing of the isotropic radiators in the aperture plane to assign I_{mn} as a function of r'. The next step is to derive $\overline{E}_{S12}(\theta, \phi=0)$.
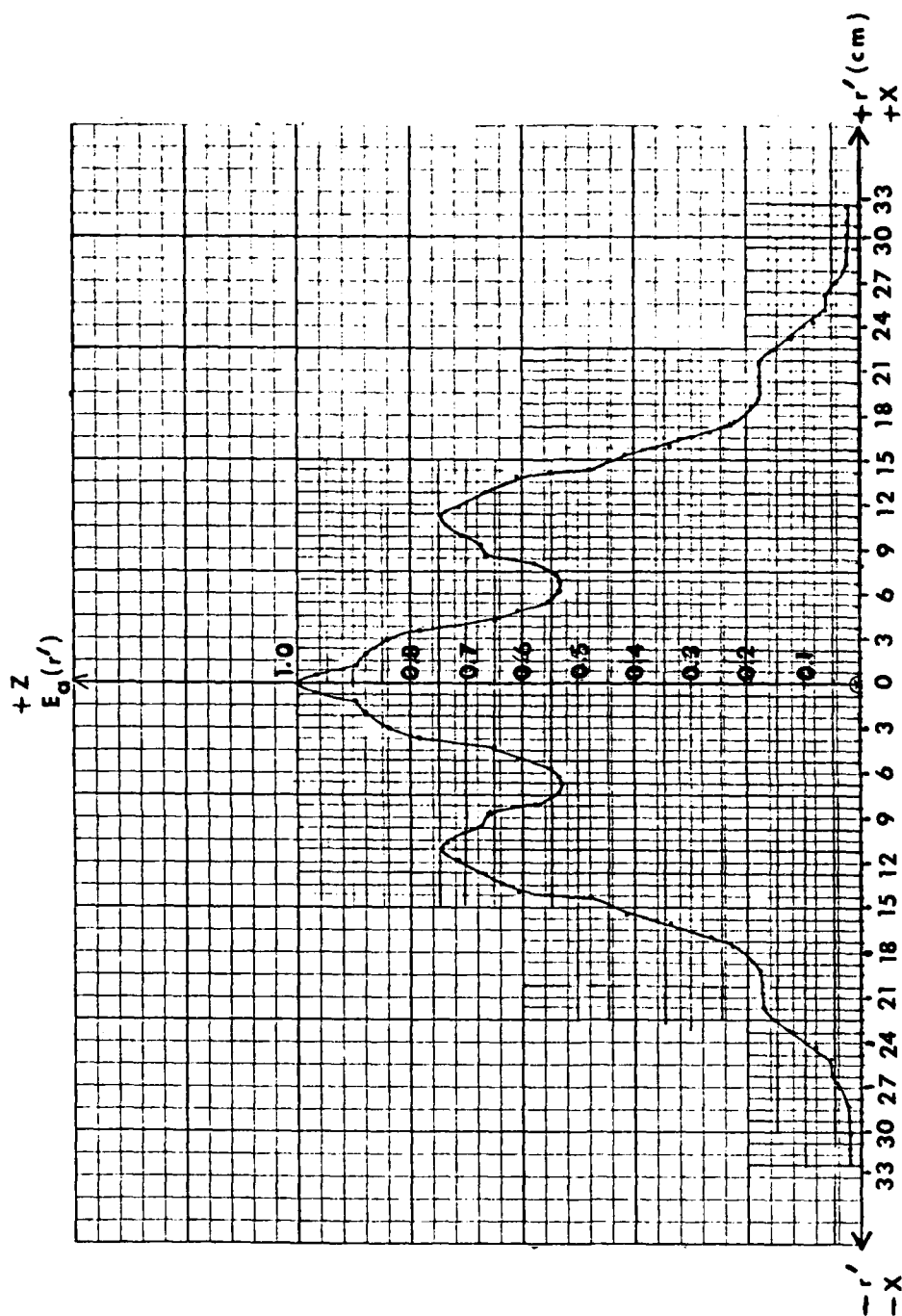
Figure 12.   Normalized Aperture Distribution

21

Physical Optics: Discs Only

The scattering by a metal disc will be derived first. For a perfectly conducting body the physical optics approximate surface currents are (Stutzman and Thiele, 1981:455):

$$\bar{J}_{PO} = \begin{cases} 2(\hat{n} \times \bar{H}_1) & \text{in illuminated region} \\ 0 & \text{in shadow region} \end{cases} \qquad (2\text{-}14)$$

Figure 13 will be used as the coordinate system in the development of $\bar{E}_{S12}(\theta, \phi=0)$ and $\bar{E}_{FB}(\theta, \phi=0)$.
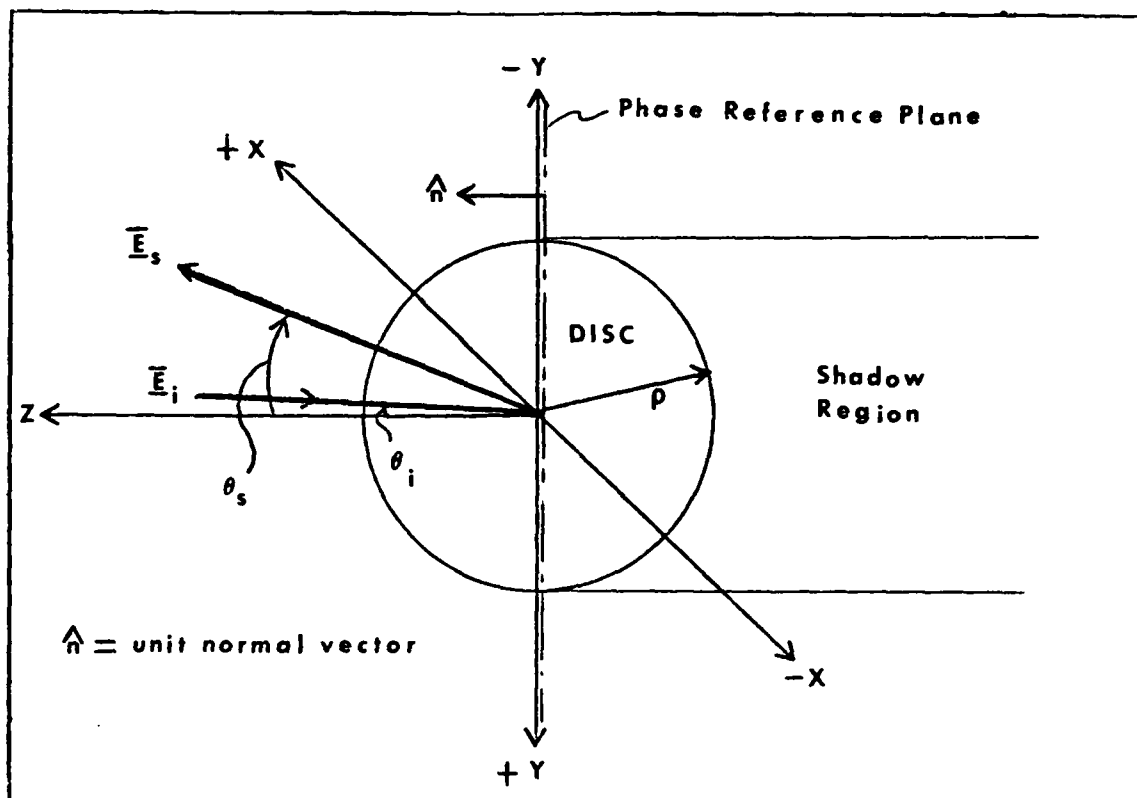
Figure 13. Coordinate System For Discs and and Feed Blockage Terms

Once $\overline{E}_{S12}(\theta, \phi=0)$ and $\overline{E}_{FB}(\theta, \phi=0)$ are developed, these terms will then be phase referenced back to the system coordinate reference, z=0 on Figure 10. Assume for now the flat metal disc lies in the xy plane, having dimensions

$$\rho = \text{disc radius}$$
$$\phi = 0^\circ \text{ to } 360^\circ$$
$$\theta = 90^\circ \text{ to } -90^\circ$$

The disc is illuminated by a plane wave from the transmitter having fields

$$\overline{E}_1(\overline{r}) = -\hat{y}E_{os}e^{-j\beta(x\sin\theta i - z\cos\theta i)} \qquad (2-15)$$

where: θ_1 = angle of incidence wrt z axis and $\hat{n}$

$\overline{r}$ = vector from origin to observation point

E_{os} = initial E-field amplitude received by disc

Assuming free space

$$\overline{H}_1(\overline{r}) = \frac{\overline{\nabla} \times \overline{E}_1(\overline{r})}{-j\omega\mu_o} \qquad (2-16)$$

Then

$$\overline{H}_1(\overline{r}) = \frac{E_{os}}{\eta_o}\left(-\hat{x}\cos\theta_1 - \hat{z}\sin\theta_1\right)e^{-j\beta(x\sin\theta i - z\cos\theta i)} \qquad (2-17)$$

where: $\eta_o = \frac{\omega\mu_o}{\beta}$

Thus the surface currents on the disc are given by the physical optics approximation

$$\overline{J}(\overline{r}') = 2\hat{n} \times \overline{H}_1(\overline{r})$$

23

since $\hat{n} = \hat{z}$ and $\hat{z} = 0$ at the surface

$$\overline{J}(\overline{r}') = -y\, \frac{2E_{os}}{\eta_o}\cos\theta_1 e^{-j\beta x \sin\theta_1} \tag{2-18}$$

Note: The physical optics approximation is not exact and is useful when

$$\rho > \lambda$$

$$\text{actual } \rho = 5 \text{ inches}$$
$$\text{actual } \lambda = 3.79 \text{ inches}$$

Neglecting effects of the edges on the surface currents, the magnetic vector potential for the scattered field can then be calculated by (Johnson, 1984)

$$\overline{A}_{ff}(\overline{r}') = \iint\limits_{\text{Source}} \frac{\mu_o \overline{J}(\overline{r}')e^{-j\beta R}}{4\pi R}\, da' \tag{2-19}$$

where: $R = |\overline{r} - \overline{r}'| \approx r - \hat{r} \cdot \overline{r}'$

$r = |\overline{r}| = $ distance from origin to observation point

$da' = \rho' d\rho'\, d\phi'$

Collecting all terms together

$$\overline{A}_{ff}(\overline{r}') = \tag{2-20}$$
$$\frac{-\hat{y}2\mu_o E_{os}e^{-j\beta r}}{\eta_o 4\pi r} \int_0^\rho\int_0^{2\pi} \cos\theta_1 e^{-j\beta x'\sin\theta_1} e^{-j\beta \overline{r}'}\cdot \hat{r}\; \rho' d\rho'\, d\phi'$$

where: $x' = \rho'\cos\phi'$

$\overline{r}' \cdot \hat{r} = \rho'\sin\theta\left[\cos\phi\cos\phi' + \sin\phi'\sin\phi\right]$

Therefore

$$\overline{A}_{ff}(\overline{r}') = \frac{-\hat{y}2\mu_o E_{os}\cos\theta_1 e^{-j\beta r}}{\eta_o 4\pi r} \tag{2-21}$$

$$\int_0^\rho\int_0^{2\pi} e^{-j\beta\rho'\sin\theta_1\cos\phi'}\, e^{j\beta\rho'\sin\theta\cos(\phi - \phi')}\; \rho' d\rho'\, d\phi'$$

24

Because of the symmetry of the disc, the scattered fields will have no ϕ dependence, set $\phi = 0$. Therefore, the two exponential exponents in Eq (2-21) can be combined and simplified to

$$e^{j\beta\rho'\left[\cos\phi'(\sin\theta - \sin\theta_i)\right]}$$

Thus rewritting Eq (2-21) and regrouping it more conviently

$$\overline{A}_{ff}(\overline{r}') = \frac{-\hat{y}\mu_0 E_{os}\cos\theta_i e^{-j\beta r}}{\eta_0 r} \tag{2-22}$$

$$\int_0^\rho \left[\frac{1}{2\pi} \int_0^{2\pi} e^{j\beta\rho'}\cos\phi'(\sin\theta - \sin\theta_i)\, d\phi'\right] \rho'\, d\rho'$$

From (Stutzman and Thiele, 1981:566)

$$J_0(x) = \frac{1}{2\pi} \int_0^{2\pi} e^{jx\cos\alpha}\, d\alpha$$

where: $J_0(x)$ is the bessel function of the zero order

Letting $x = \beta\rho'(\sin\theta - \theta_i)$ and $\alpha = \phi'$

$$\overline{A}_{ff}(\overline{r}') = \frac{-\hat{y}\mu_0 E_{os}\cos\theta_i e^{-j\beta r}}{\eta_0 r} \int_0^\rho \rho' J_0\left[\beta\rho'(\sin\theta - \sin\theta_i)\right] d\rho' \tag{2-23}$$

From (Stutzman and Thiele, 1981:566)

$$xJ_1(x) = \int xJ_0(x)dx$$

where: $J_1(x)$ is the bessel function of the first order.

Letting $x = \beta\rho'(\sin\theta - \sin\theta_i)$ then $dx = \beta(\sin\theta - \sin\theta_i)d\rho'$ therefore

$$\overline{A}_{ff}(\overline{r}') = \frac{-\hat{y}\mu_0 E_{os}\cos\theta_i e^{-j\beta r}}{\eta_0 r\beta(\sin\theta - \sin\theta_i)^2} \int_0^\rho xJ_1(x)dx \tag{2-24}$$

25

Finally

$$\overline{A}_{ff}(\overline{r}') = \frac{-\hat{\theta}2A\mu_0E_{os}\cos\theta_1 e^{-j\beta r}}{\eta_0 2\pi r} \ J_1\left|\frac{\beta\rho(\sin\theta - \sin\theta_1)}{\beta\rho(\sin\theta - \sin\theta_1)}\right| \qquad (2\text{-}25)$$

where: A = area of disc

Again

$$\overline{E}_{S1}(\theta,\phi=0) \approx -j\omega\overline{A}_{ff}(\overline{r}') \qquad \qquad \text{disregarding the radial component}$$

where: $\overline{E}_{S1}(\theta,\phi=0)$ is the complex E-field scattering off one disc.

Simplifying and combining all terms yields

$$\overline{E}_{S1}(\theta,\phi=0) \approx \frac{\hat{\theta}jE_{os}\beta e^{-j\beta r}\cos\theta_1}{2\pi r}\left(2A \ \frac{J_1(x)}{x}\right) \qquad (2\text{-}26)$$

where: $x = \beta\rho(\sin\theta - \sin\theta_1)$

How is this modified for two movable discs on the reflector

for $\phi = 0$ i.e. (the H-plane cut), see Figure 14 next page?
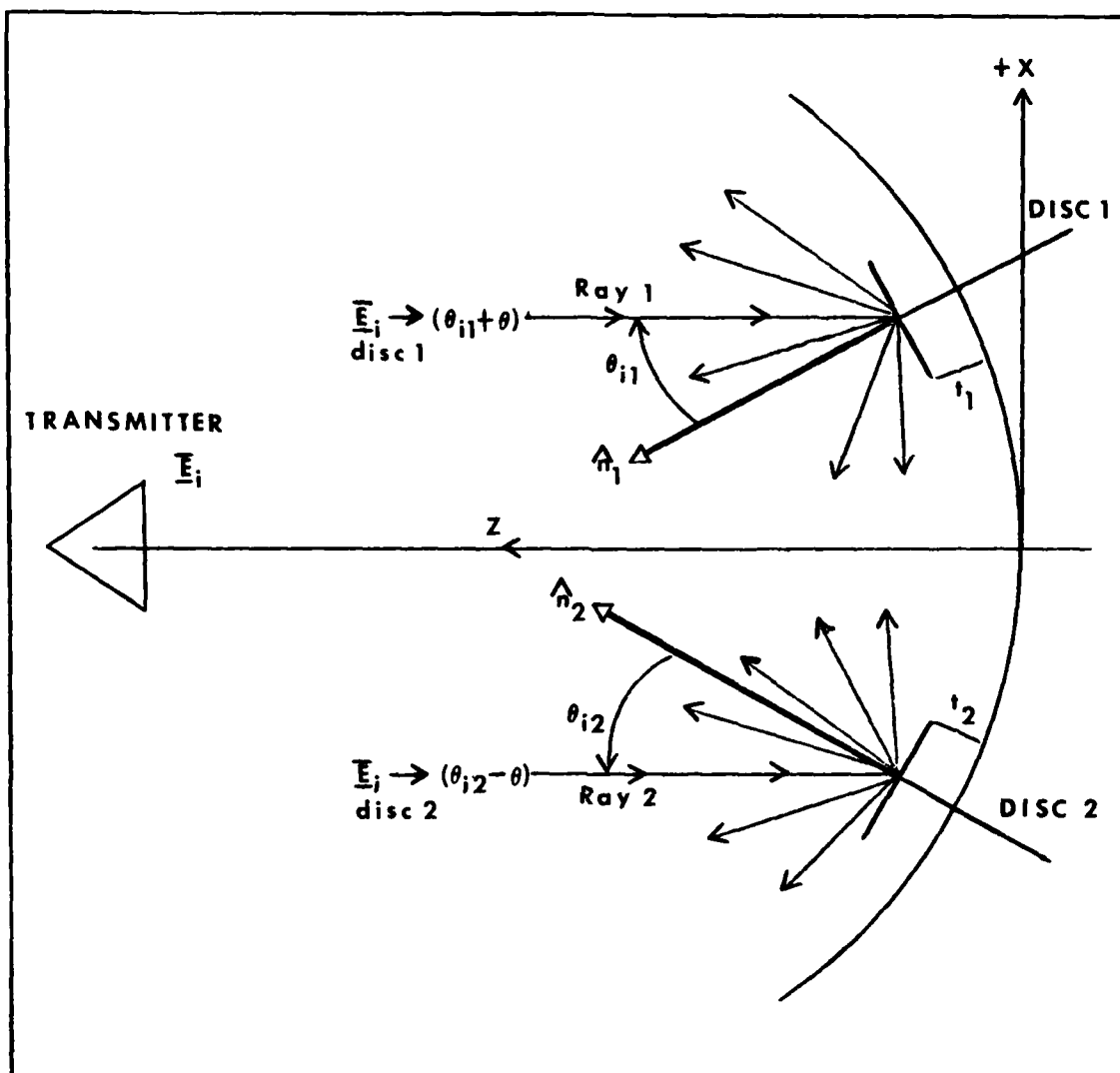
Figure 14.   H-plane Cut of Antenna System

Since the discs are movable, the phase or path length difference
between $\overline{E}_{i(disc1)}$ will be different from $\overline{E}_{i(disc2)}$ when
$t_1 \neq t_2$.   Expanding the picture on disc 1 to develop the
path length difference (phase) associated with changing t_1,
will lead to the phase term to add onto Eq (2-26) to account

for changing phase due to changes in both t_1 and t_2.

From Figure 15 (neglecting double diffractions, moding, and edge effects), $\overline{E}_{ib}$ travels approximately $t_1\cos\theta_{i1} + t_1\cos(\theta_{i1} + \theta)$ · farther than $\overline{E}_{ia}$.
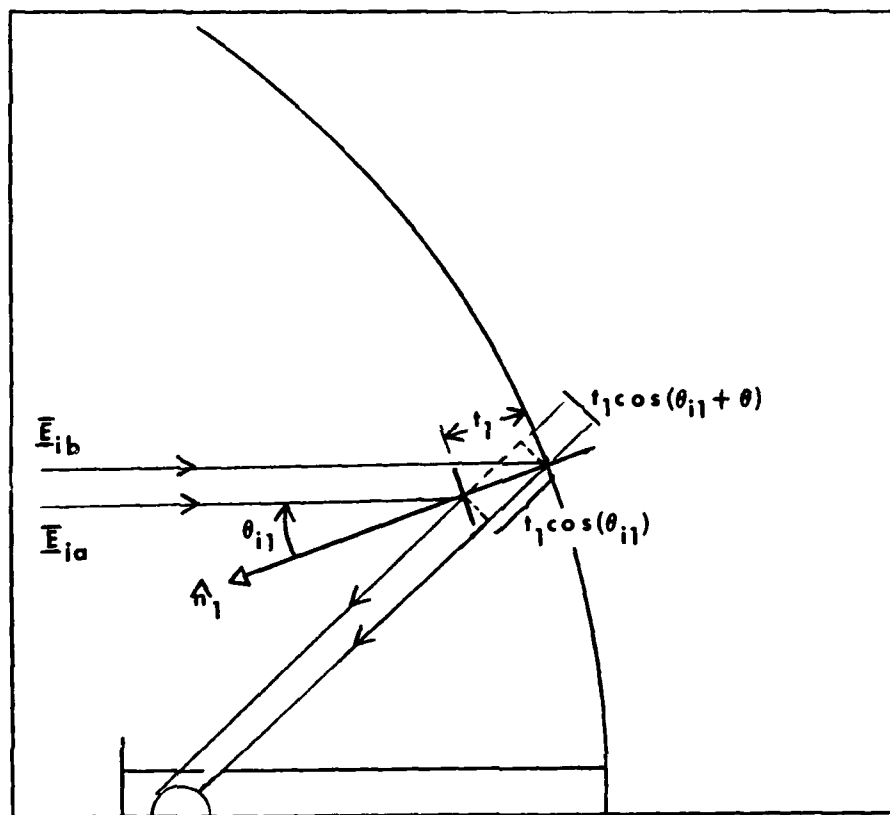
Figure 15.   Phase Difference Due to Movable Disc

Using array theory to look at the phase differences between $\overline{E}_{ia}$ and $\overline{E}_{ib}$ and after a multitude of algebra steps, the

phase difference can be expressed as (Rudduck, 1985a)

$$\left\{ e^{j\beta t1 \left[\left(\cos\theta_{11} + \cos(\theta_{11} + \theta) \right) \right]} - 1 \right\}$$

But since there are two discs the phase term must reflect this

$$\left\{ e^{j\beta t_{\frac{1}{2}} \left[\left(\cos\theta_{1\frac{1}{2}} + \cos(\theta_{1\frac{1}{2}} \pm \theta) \right) \right]} - 1 \right\}$$

where: subscript 1 represents disc 1 and
              subscript 2 represents disc 2

After further algebraic manipulation the phase term associated
with Eq (2-26) for both discs in the H-plane becomes

$$2j \left| \sin\left[\frac{\beta t_1}{2} \left(\cos\theta_{11} + \cos(\theta_{11} + \theta) \right) \right] e^{j\frac{\beta t_1}{2} \left[\cos\theta_{11} + \cos(\theta_{11} + \theta) \right]} \right.$$

$$\left. + \sin\left[\frac{\beta t_2}{2} \left(\cos\theta_{12} + \cos(\theta_{12} - \theta) \right) \right] e^{j\frac{\beta t_2}{2} \left[\cos\theta_{12} + \cos(\theta_{12} - \theta) \right]} \right|$$

$$e^{j\beta w\cos\theta}$$

where: $e^{j\beta w\cos\theta}$ is added to reference the phase term back
              to the system coordinate phase reference (see Figure 10)

Finally since the area of disc 1 equals the area of disc 2 and $|\theta_{i1}| = |\theta_{i2}|$ so that θ_i is considered always (+), the final expression for scattering off the discs is:

$$
\overline{E}_{S12}(\theta, \phi=0) \approx \hat{\theta} E_{os} \beta e^{-j\beta r} e^{j\beta w \cos\theta} \frac{(\cos\theta_i) A}{\pi r} \qquad (2-27)
$$

$$
\left\{ \frac{2J_1 \left[\beta\rho_o(\sin\theta + \sin\theta_i)\right]}{\beta\rho_o(\sin\theta + \sin\theta_i)} \right.
$$

$$
\left(\sin\left[\frac{\beta t_1}{2}\left(\cos\theta_i + \cos(\theta_i + \theta)\right)\right] e^{j\frac{\beta}{2}t_1\left[\cos\theta_i + \cos(\theta_i + \theta)\right]}\right)
$$

$$
+ \frac{2J_1 \left[\beta\rho_o(\sin\theta - \sin\theta_i)\right]}{\beta\rho_o(\sin\theta - \sin\theta_i)}
$$

$$
\left. \left(\sin\left[\frac{\beta t_2}{2}\left(\cos\theta_i + \cos(\theta_i - \theta)\right)\right] e^{j\frac{\beta}{2}t_2\left[\cos\theta_i + \cos(\theta_i - \theta)\right]}\right)\right\}
$$

see Appendix A for actual values for

θ_{i1}, θ_{i2}, w, A, E_{os}, r, λ, ρ_o

Physical Optics: Feed Blockage Only

A good approximation to feed blockage effects is to subtract the radiation pattern of the parasitic reflector from the radiation pattern of the parabolic reflector. Depending on the angle, the feed will block a portion of the radiation causing a "shadow" on the reflector surface. The feed can be modeled as a disc with an area equal to that of the circular parasitic reflector (see Figure 3). Then for the E-field scattered off one disc, Eq (2-26) can be used with θ_i equal to 0.

$$\bar{E}_{FB}(\theta,\phi=0) \simeq \frac{\hat{\phi} j E_{ofb} B e^{-j\beta r} e^{j\beta q \cos\theta}(\beta)}{2\pi r}\left(\frac{2J_1(\beta r_o \sin\theta)}{\beta r_o \sin\theta}\right) \qquad (2-28)$$

where: r_o = radius of parasitic reflector

   B = area of parasitic reflector

   E_{ofb} = the initial E-field amplitude
            received by parasitic reflector

   $e^{j\beta q \cos\theta}$ = is added to reference the phase back to
            the system coordinate phase reference
            (see Figure 10)

see Appendix A for actual values for

E_{ofb}, r_o, B, r

III. Analysis and Results

Computer Programs

Three Fortran-77 programs (see Appendix C) are used to produce relative power patterns (Program PHASENUL), and field intensity amplitudes and phase plots for the discs alone (Program PHASCANL), and the dish alone (Program PHASEQ). Program PHASENUL calculates $|\overline{E}_{TOT}(\theta,\phi=0)|^2$ which is proportional to the relative power pattern of the antenna system (see Figures 16-27).

$$|\overline{E}_{TOT}(\theta,\phi=0)|^2 = |\overline{E}_D(\theta,\phi=0) + \overline{E}_{S12}(\theta,\phi=0) - \overline{E}_{FB}(\theta,\phi=0)|^2$$

where: $\overline{E}_D(\theta,\phi=0)$ = Eq (2-12)

$\overline{E}_{S12}(\theta,\phi=0)$ = Eq (2-27)

$\overline{E}_{FB}(\theta,\phi=0)$ = Eq (2-28)

Program PHASCANL calculates the amplitude and phase of the field intensity of the discs alone which is proportional to $|\overline{E}_{(C)cancellation}(\theta,\phi=0)|$ (see Figures 30,31).

$$|\overline{E}_C(\theta,\phi=0)| = |\overline{E}_{S12}(\theta,\phi=0)| \qquad (3-1)$$

Program PHASEQ calculates the amplitude and phase of the field intensity of the dish alone which is proportional to $|\overline{E}_{(Q)quiescent}(\theta,\phi=0)|$ (see Figures 28,29).

$$|\overline{E}_Q(\theta,\phi=0)| = |\overline{E}_D(\theta,\phi=0) - \overline{E}_{FB}(\theta,\phi=0)| \qquad (3-2)$$

Results

When $|\overline{E}_C(\theta,\phi=0)|$ is multiplied by its phase and $|\overline{E}_Q(\theta,\phi=0)|$ is multiplied by its phase, and the two terms added together, $|\overline{E}_{TOT}(\theta,\phi=0)|$ results. $|\overline{E}_{TOT}(\theta,\phi=0)|^2$ is obtained by squaring the real part, adding the square of the imaginary part, normalizing, and plotting in dB. By breaking $|\overline{E}_{TOT}(\theta,\phi=0)|^2$ into $|\overline{E}_C(\theta,\phi=0)|$ and $|\overline{E}_Q(\theta,\phi=0)|$ the phase cancelling in the side lobes of the quiescent H-plane pattern of the dish by the discs is more apparent. This will be discussed in the conclusion section.

The results of the computer programs and actual measured power patterns follow. For comparison purposes, the measured power pattern is shown first followed by the theoretical pattern for the same disc positions. The system quiescent power pattern is generated with the two discs flush on the reflector surface. Appendix D shows the actual disc positions that were used to produce a measured pattern at a specific null angle (θ). The PHASENUL program uses the actual disc positions to produce the theoretical patterns. Following the power patterns are the theoretical field intensity plots. There are no actual measured plots for comparison. The amplitudes of the field intensity plots are not normalized, to show that the cancellation effects of the discs occur at the sidelobe level of the reflector.

33
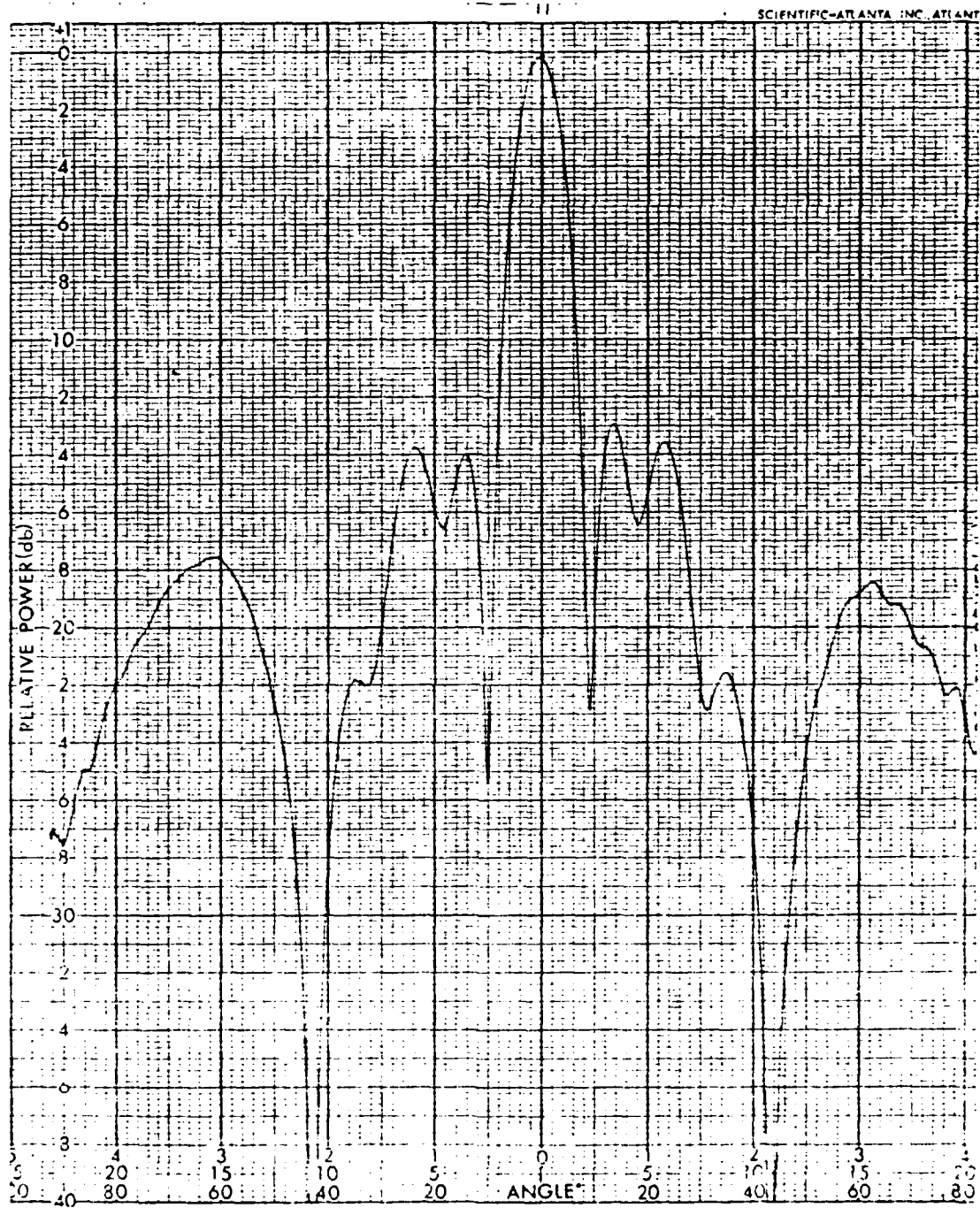
Figure 16. Measured Unmodified H-plane Power Pattern

SYSTEM
QUIESCENT POWER PATTERN
TWO FOOT PARABOLIC REFLECTOR
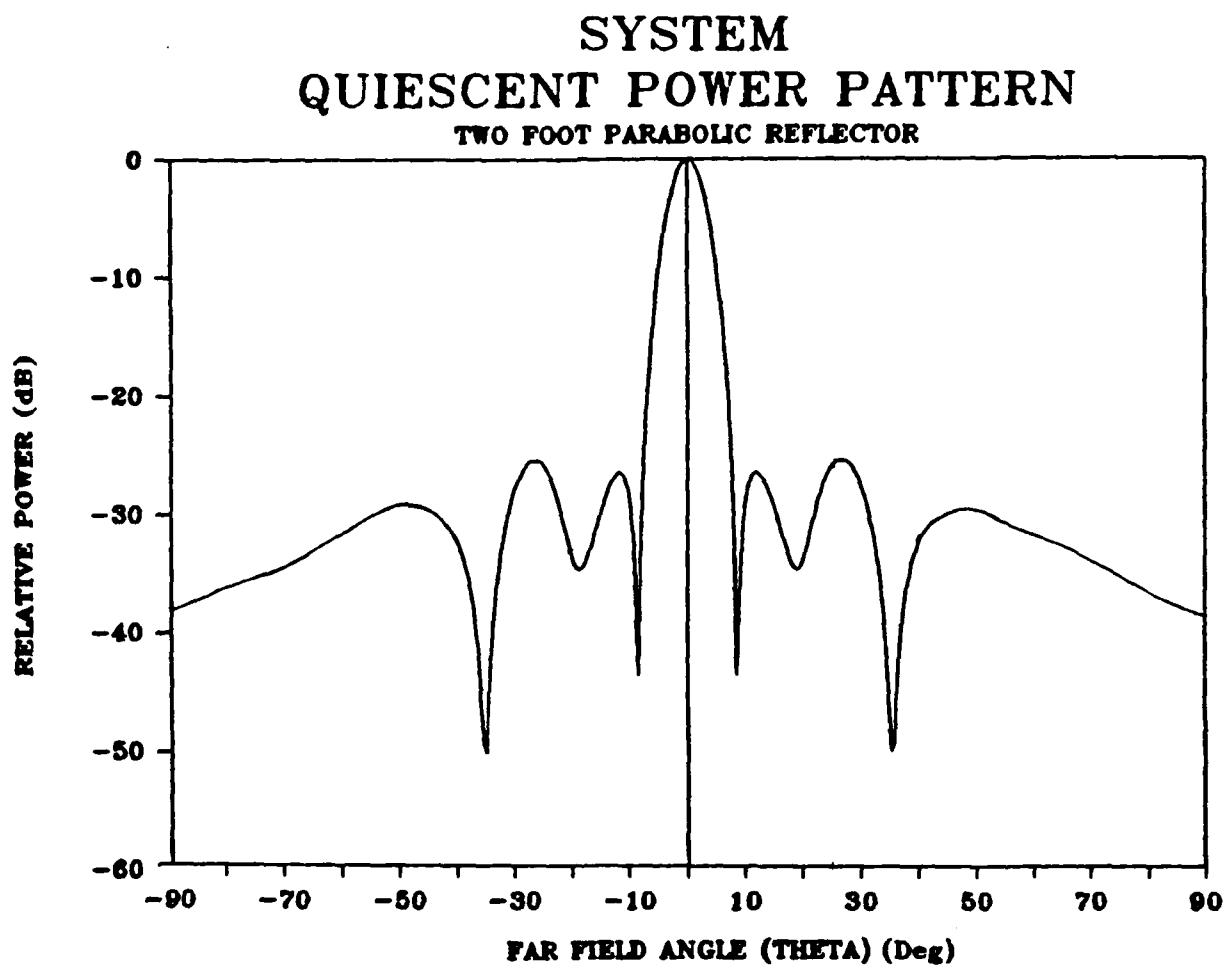
Figure 17.   Theoretical Unmodified H-plane Power Pattern

Figure 18.   Measured H-plane Power Pattern, System Null
θ = +35°

36
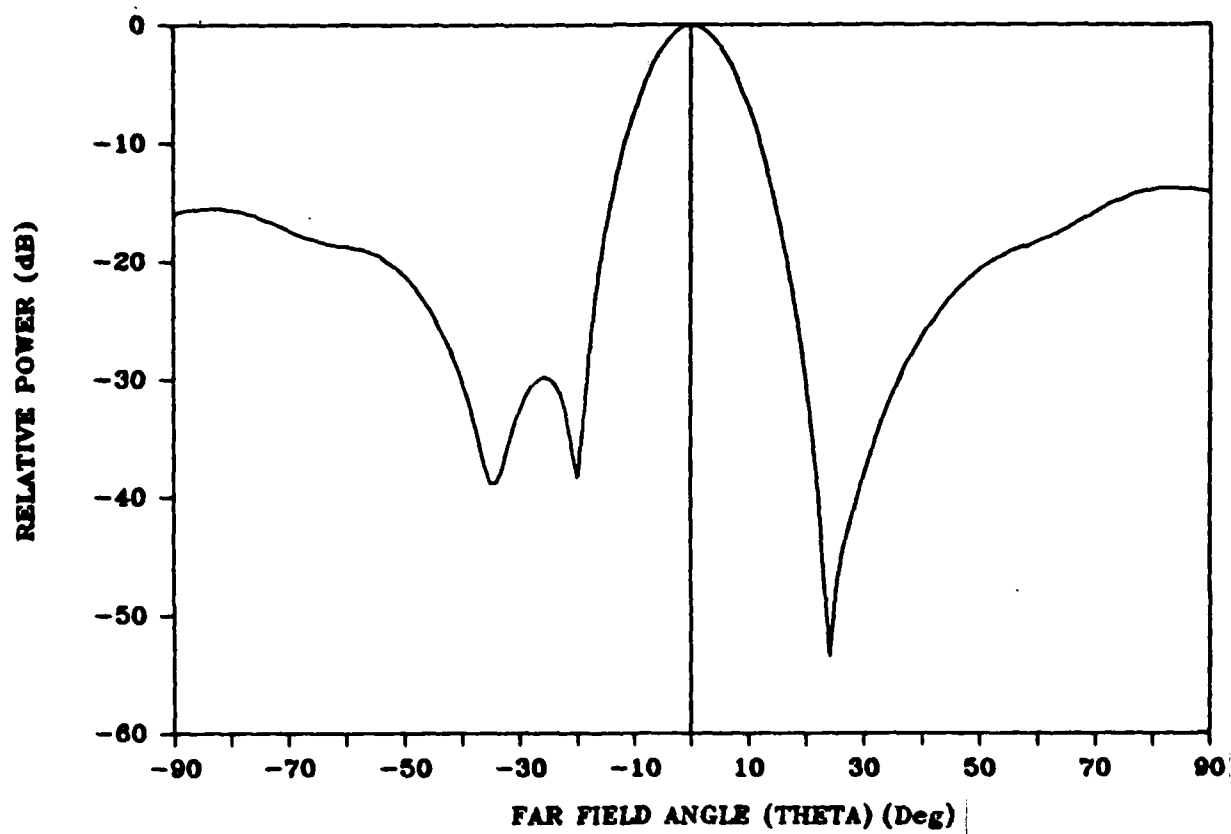
Figure 19.   Theoretical H-plane Power Pattern, System Null
$\theta = +35^\circ$

37
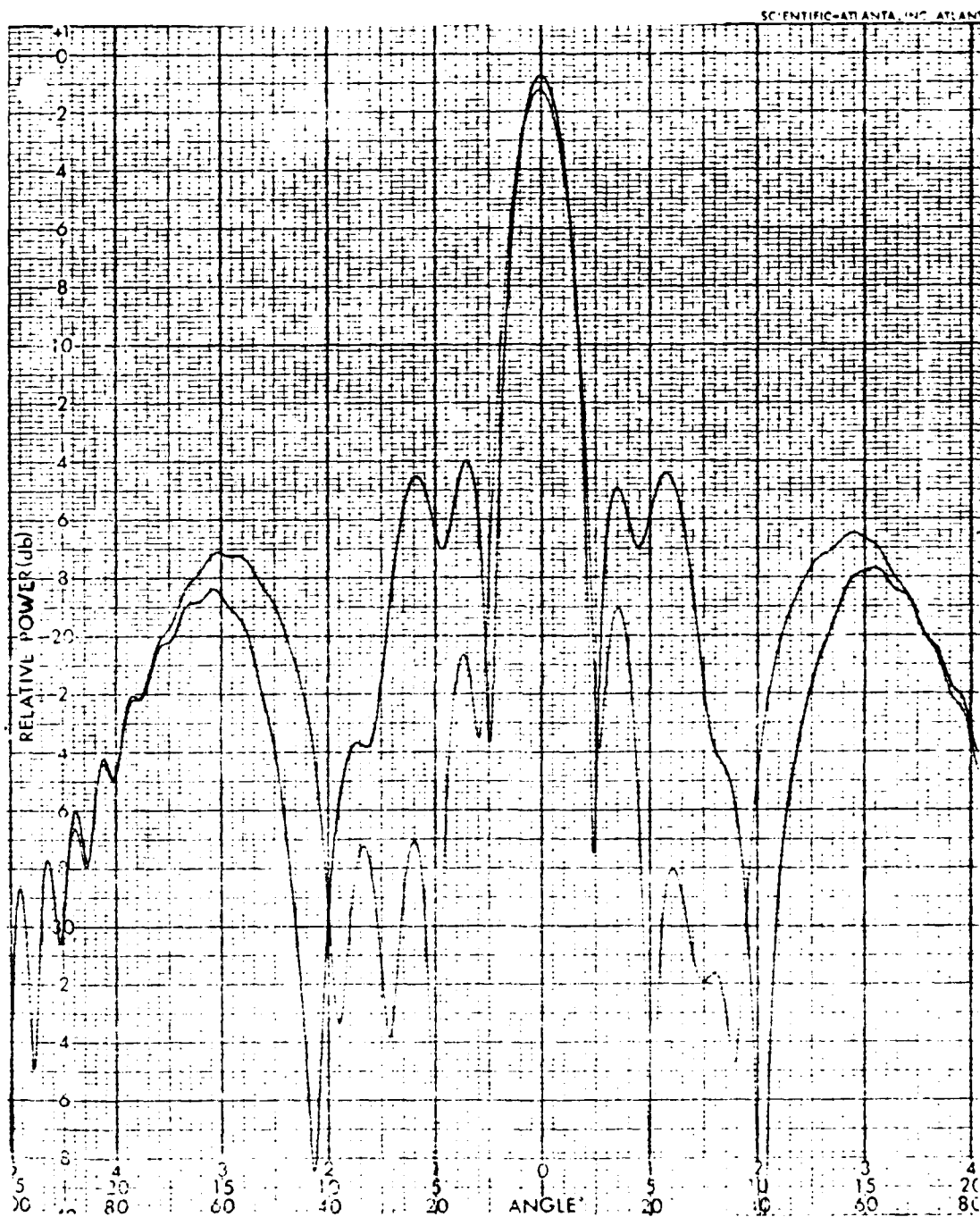
Figure 20. Measured H-plane Power Pattern, System Nulls
θ = -20°, +20°
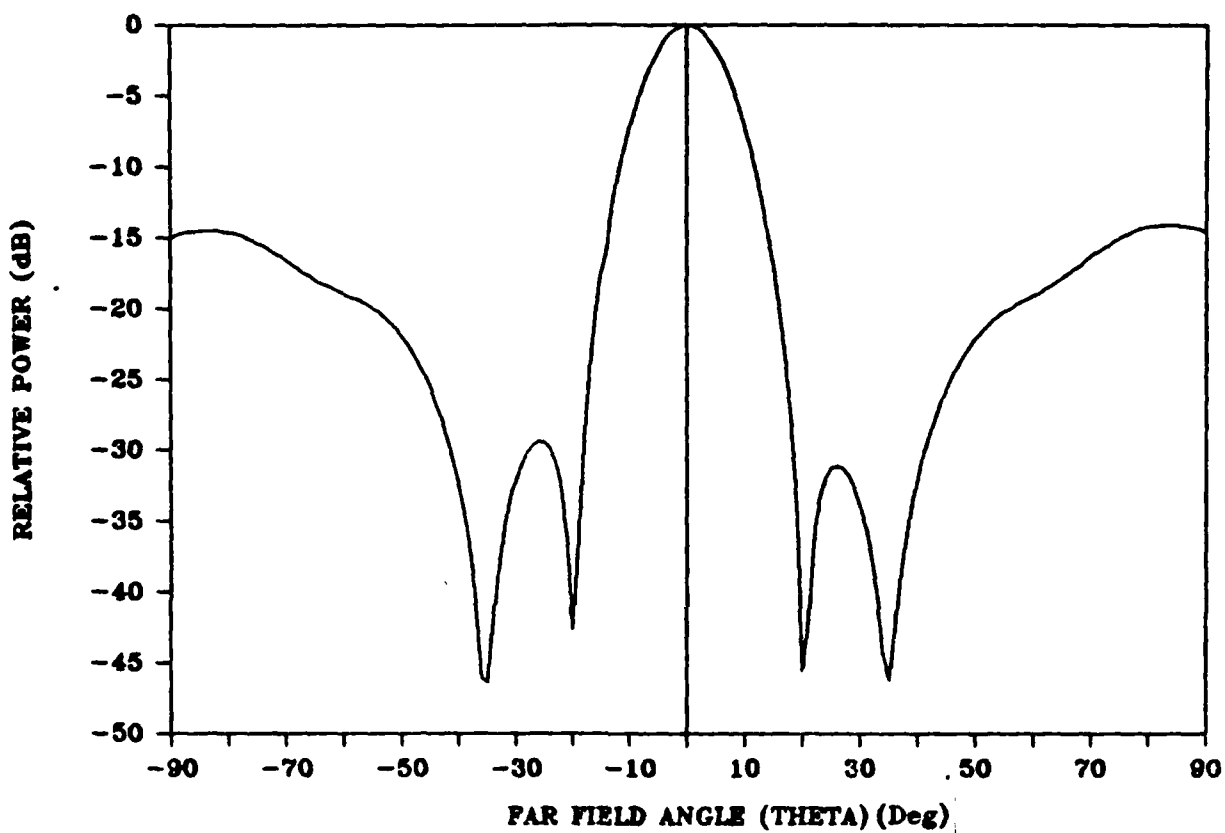
Figure 21.   Theoretical H-plane Power Pattern, System Nulls
θ = -20°, =20°

Figure 22.   Measured H-plane Power Pattern, System Null
             $\theta = -35^\circ$
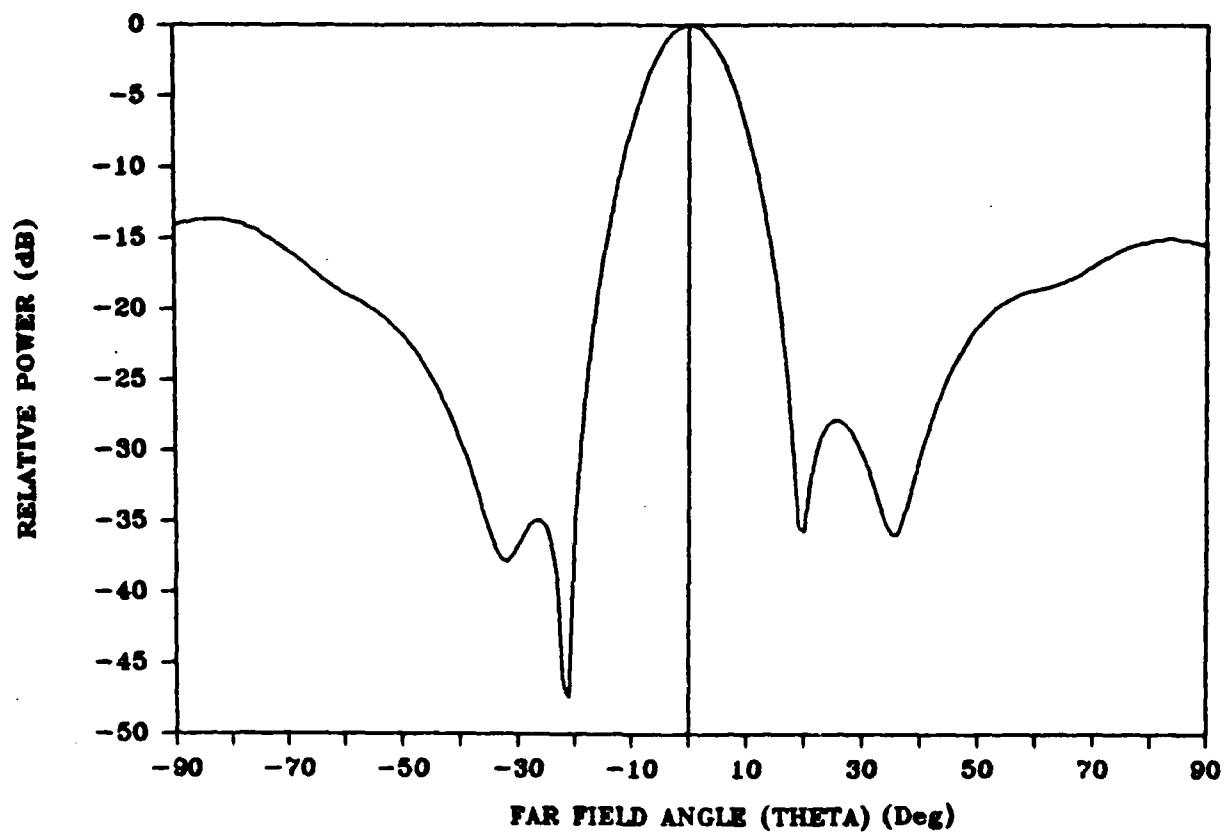
Figure 23. Theoretical H-plane Power Pattern, System Null
$\theta = -35^{\circ}$
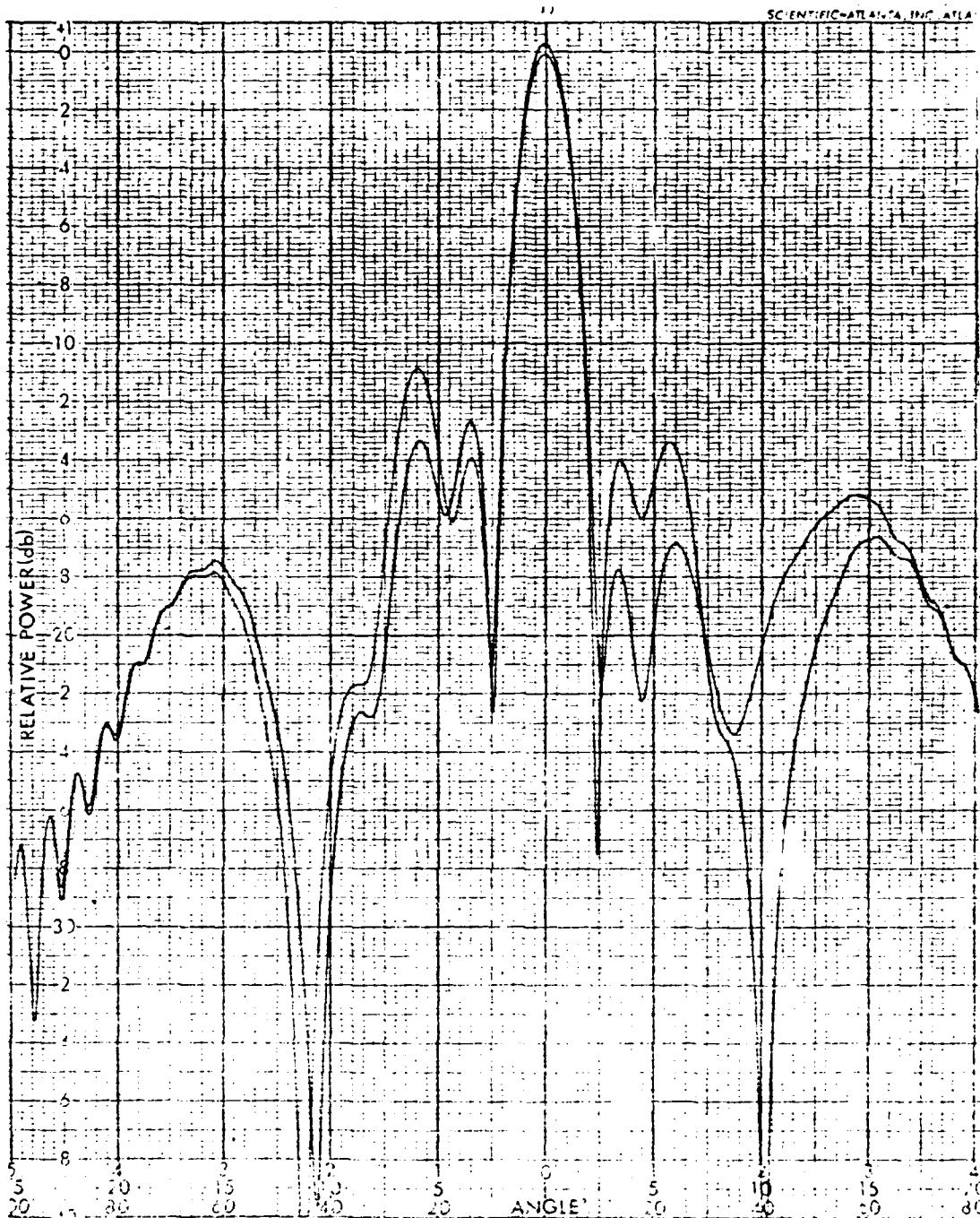
Figure 24. Measured H-plane Power Pattern, System Null
$\theta = -45°$

42
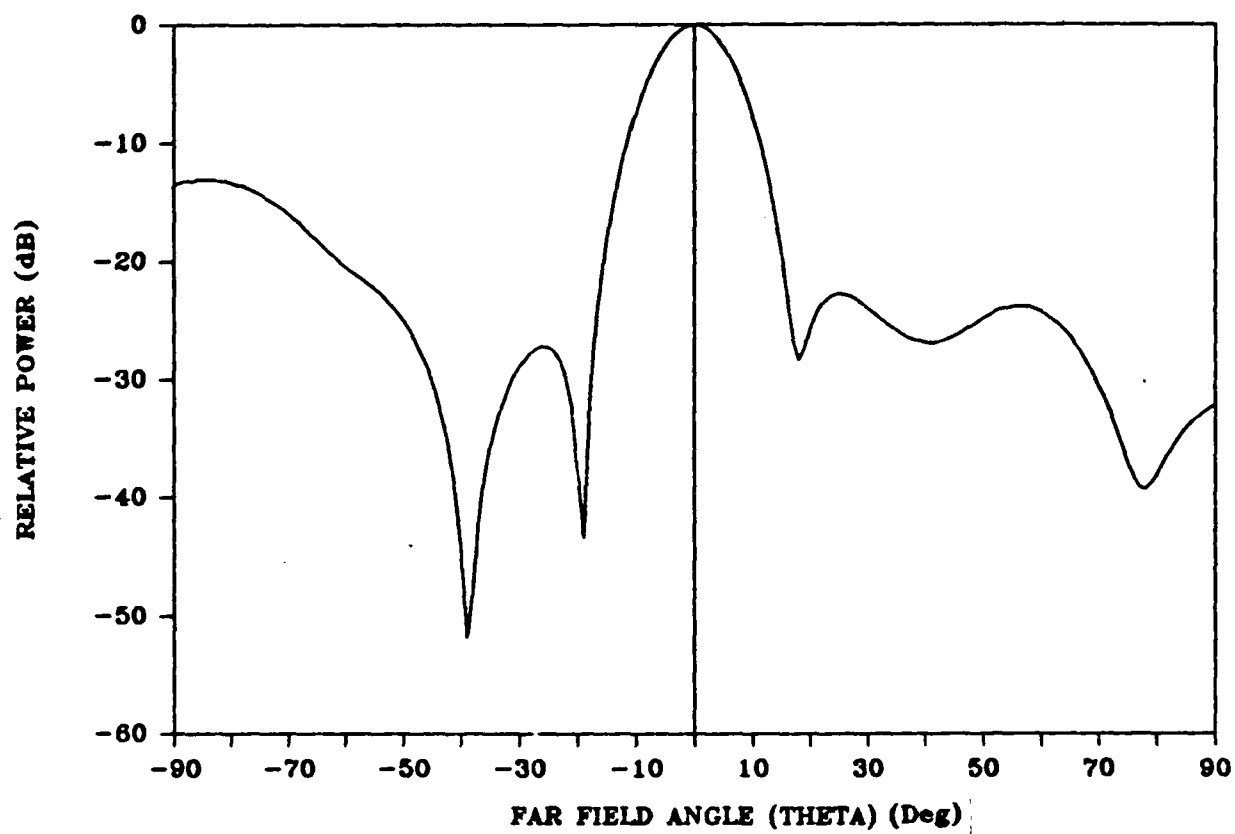
Figure 25. Theoretical H-plane Power Pattern, System Null
$\theta = -45^{\circ}$

43
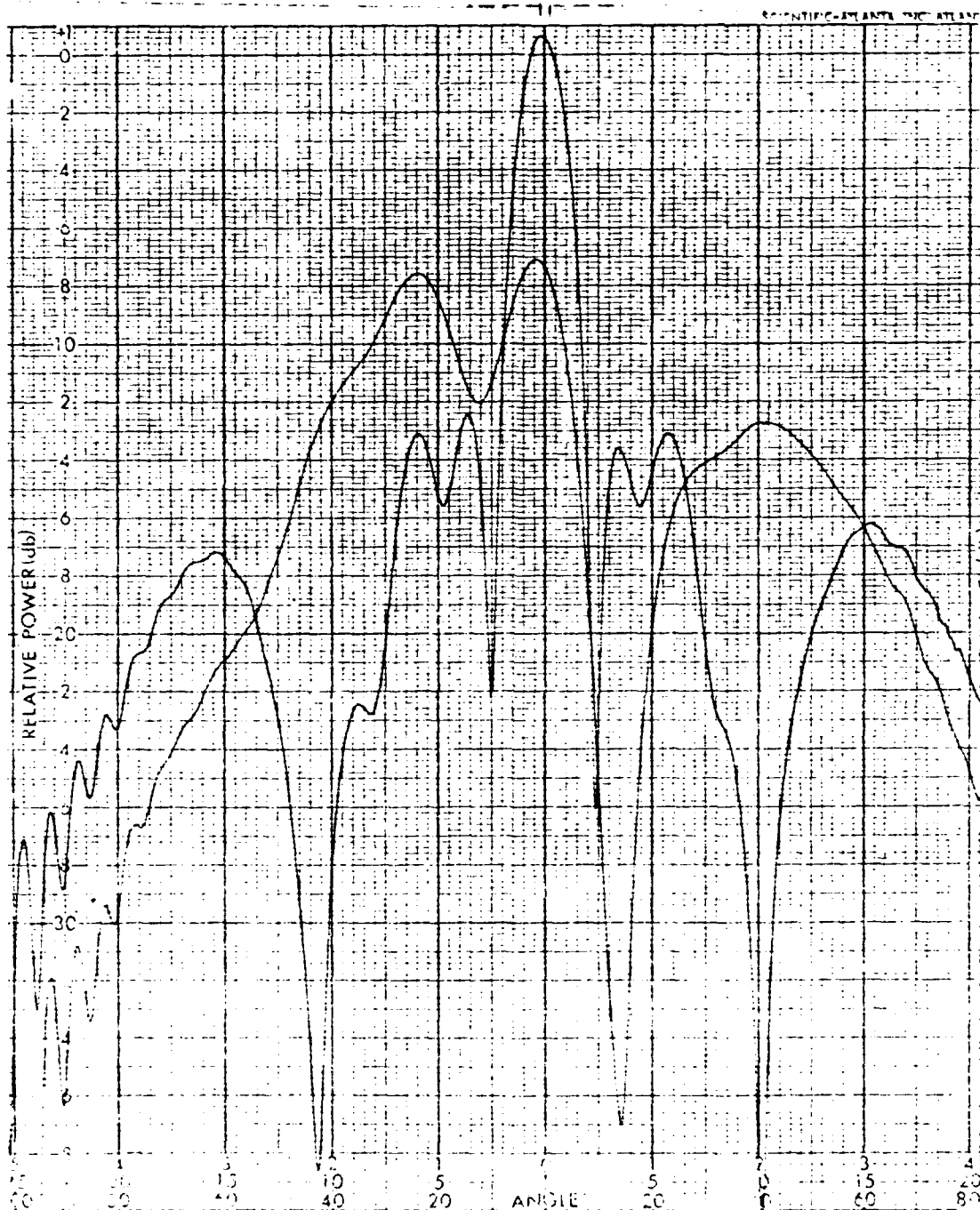
Figure 26. Measured H-plane Power Pattern, System Null
$\theta = -60°$

44
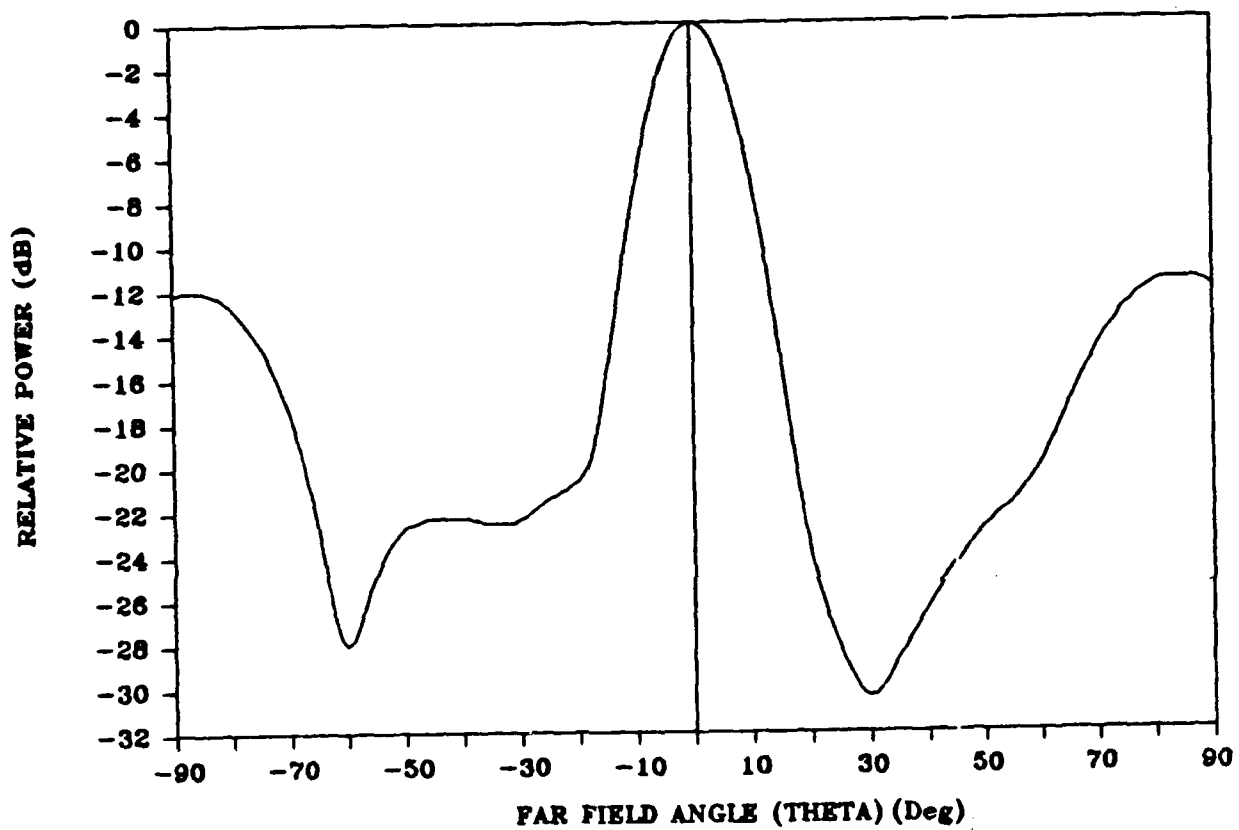
Figure 27.   Theoretical H-plane Power Pattern, System Null
$\theta = -60°$

45
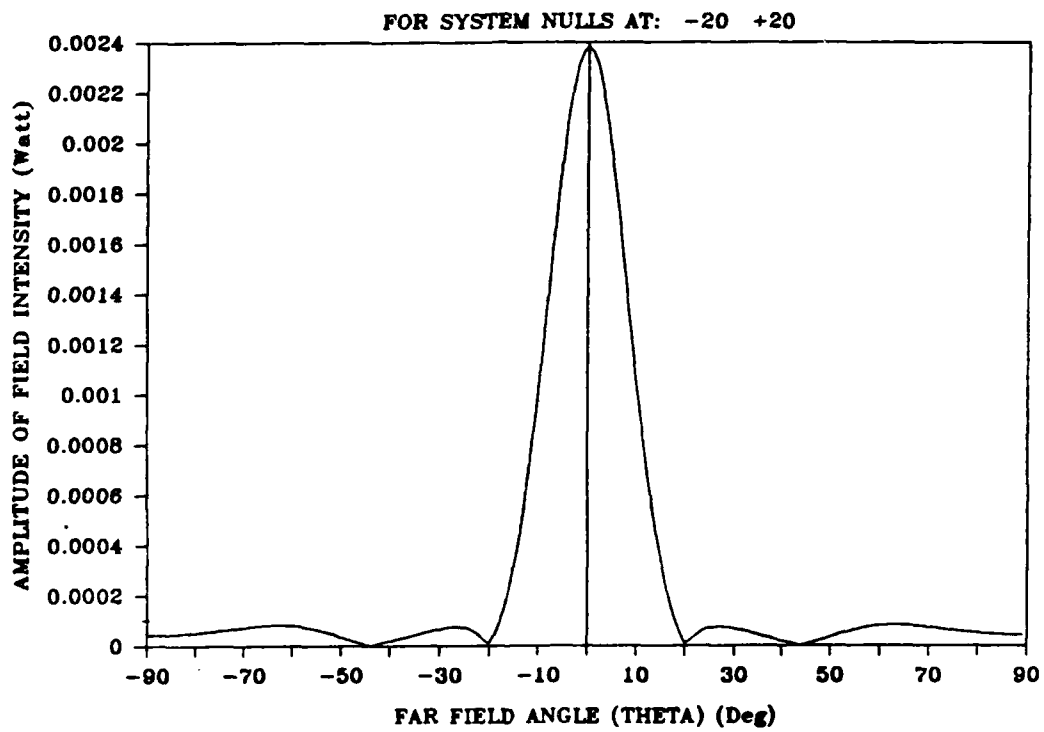
Figure 28. Theoretical Amplitude of H-plane (Dish and Feed Blockage Only): Quiescent Pattern

FOR SYSTEM NULLS AT: −20 +20
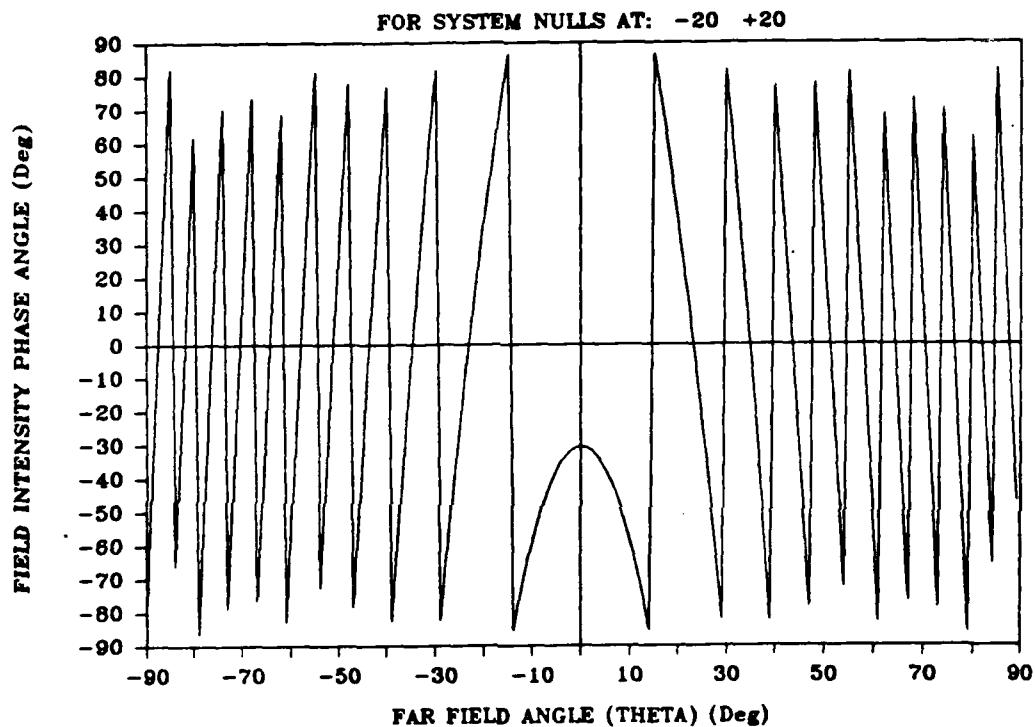
Figure 29. Theoretical Phase of H-plane (Dish and Feed
Blockage Only): Quiescent Pattern

Note: When real part of field intensity negative or when
real and imaginary part of field intensity negative
add 180° to phase angle due to properties of
arctan function used in graph above.

FOR SYSTEM NULLS AT: −20 +20
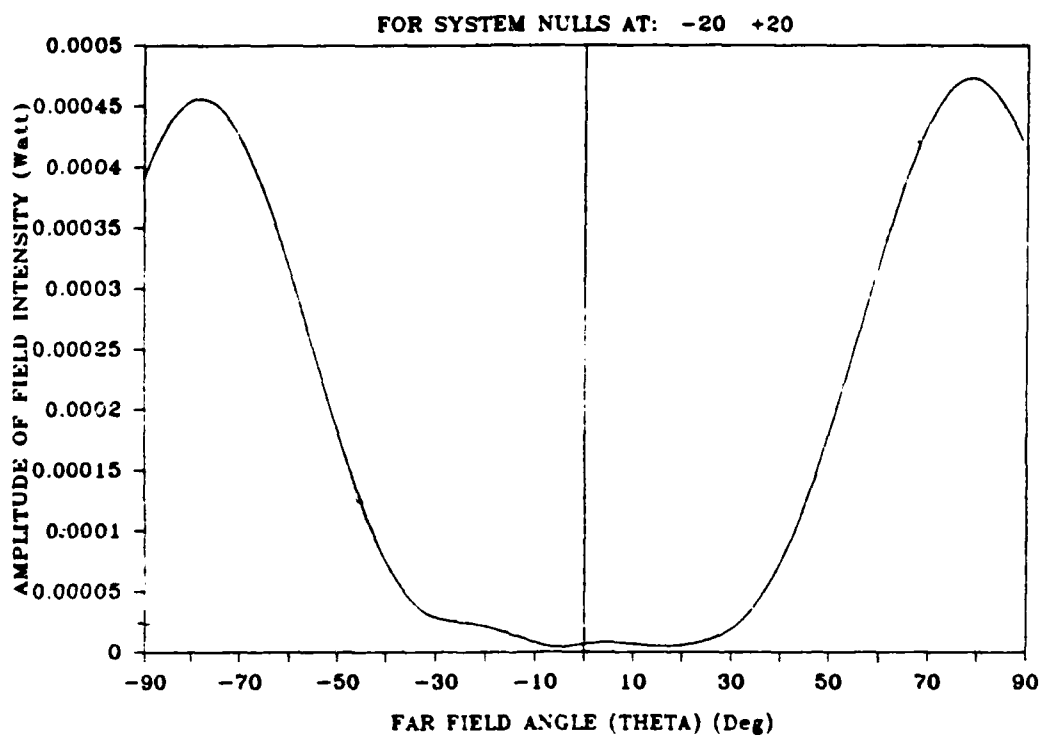
Figure 30. Theoretical Amplitude of H-plane (Discs Only)
Cancellation Pattern

48

FOR SYSTEM NULLS AT: −20 +20
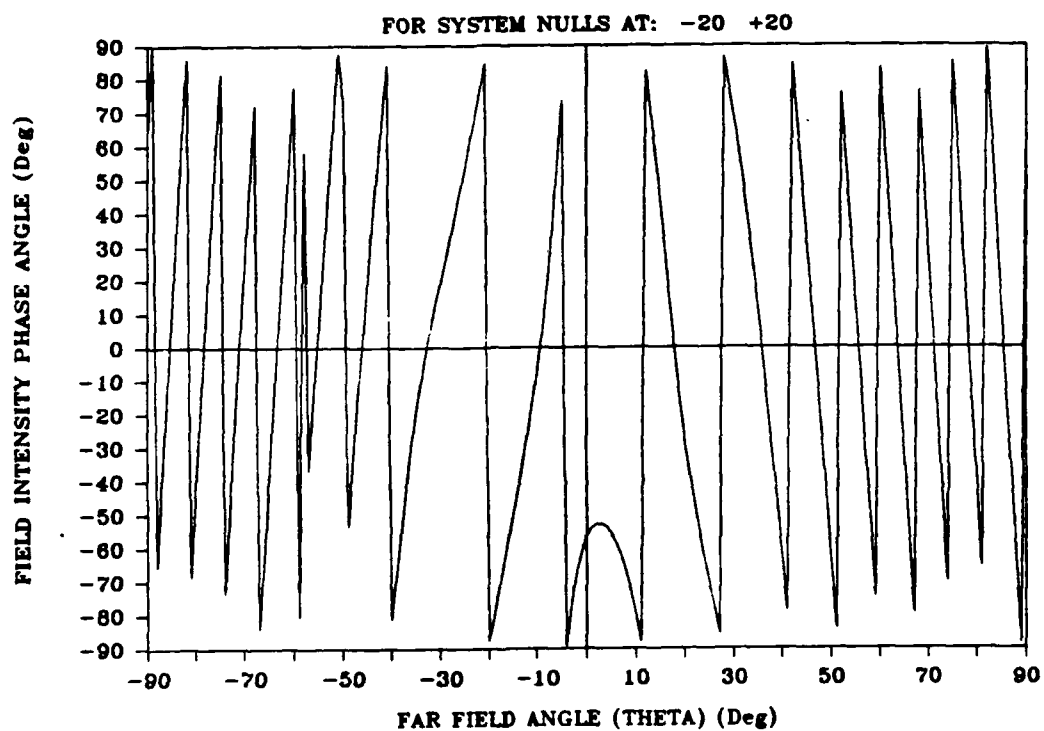
Figure 31. Theoretical Phase of H-plane (Discs Only)
Concellation Pattern

Note: When real part of field intensity negative or when
real and imaginary part of field intensity negative
add 180° to phase angle due to properties of
arctan function used in graph above.

49

IV. Conclusions

Comparisons of Theoretical to Actual Patterns

The system quiescent power pattern Figure 17 compares favorably with the actual pattern Figure 16. The theoretical power pattern side lobe levels are down considerably from the actual ones. This is a result of an idealistic model, i.e. no interference sources such as edge illumination or diffraction are included. For all theoretical power patterns, the 3dB beam widths, null placements, average far-out side lobes, and spillover radiation regions agree quite well with actual. However, the first side lobes are smeared into the main beam. This occurs because the phase distribution across the aperture is not constant and the model is not detailed enough for diffraction and double reflection effects (Skolnik, 1962:261). The goal of the model is successful; it duplicates system nulls (within $\pm$ 5° of actual), when the actual measured disc position at a specific system null angle is used in the computer program PHASENUL. Cancellation up to 25dB, along with minimum main beam degradation and minumum distortion of the overall far field pattern, is evident in the theoretical patterns matching the actual patterns. Especially successful is Figure 21. This theoretical pattern shows the symmetric nulling effects of the actual pattern Figure 20 and predicts the system nulls exactly! Acccording to Jacavanco, this was the first time he had seen symmetric nulls for a movable disc system (Jacavanco, 1985c). For all theoretical patterns the intensity or relative depth of

a null in dB (unmodified minus modified), cannot readily be compared to actual. Again this is a result of an idealistic side lobe level in the theoretical patterns.

A requirement of any nulling technique is that no main beam corruption occur such as in Figure 26. From actual measurements, main beam degradation does not occur for this system until the system null angle exceeds approximately 50°. Looking at Figure 26 this is evident. The system is set up to produce a system null at -60° but disc placement is such that they overshadow the feed arm significantly and edge illumination effects completely destroy the integrity of the pattern. The matching theoretical pattern Figure 27, while not showing pattern distortion, produces no nulls and a very unreasonable overall pattern for a parabolic dish. In larger movable disc systems that use a larger ratio of focal length to diameter (aspect ratio) and a horn feed, main beam distortion effects are less prevalent for system null angles beyond 50°.

As mentioned before, cancellation effects are more apparent by using the field intensity graphs. From Eq (2-2), the example on the next page shows how to compute a power point from the field intensity graphs, for a system null angle of (θ) = -20° from Figure 21.

(1) Eq (2-2): $\sqrt{P_{RJQ}}e^{j\phi_1} + \sqrt{P_{RJD}}e^{j\phi_2} \approx 0$

From side
lobe level
of dish

(2) $\sqrt{P_{RJQ}} \sim |\overline{E}_Q(\theta,\phi=0)|$ --> see Figure 28
at $\theta = -20°$

$\sqrt{P_{RJQ}} \approx 9 \times 10^{-6}$

From discs

(3) $\sqrt{P_{RJD}} \sim |\overline{E}_C(\theta,\phi=0)|$ --> see Figure 30
at $\theta = -20°$

$\sqrt{P_{RJD}} \approx 2 \times 10^{-5}$

(4) ϕ_1 = phase of P_{RJQ} --> see Figure 29

$\phi_1 \approx 218°$

(5) ϕ_2 = phase of P_{RJD} --> see Figure 31

$\phi_2 \approx 92°$

(6) Substituting into Eq (2-2):

$(9 \times 10^{-6})e^{j218°} + (2 \times 10^{-5})e^{-j92°} = \underbrace{7.9 \times 10^{-6}}_{a} - \underbrace{j1.6 \times 10^{-5}}_{b}$

(7) $a^2 + b^2 \sim$ power, then normalizing using the maximum
value at $\theta = 0$ yields:

5.6×10^{-5} watts

(8) Converting this to dB yields: -42.5dB

Looking at Figure 20 for the actual system null at $\theta = -20°$,
-42.5dB compares very well with a measured value of -40dB.
Ideally the discs can be positioned so $\sqrt{P_{RJQ}} = \sqrt{P_{RJD}}$ and ϕ_1
is 180° out of phase with ϕ_2. However, in practice this
would represent "perfect" cancellation which is impossible due
to secondary effects. In addition, null depths beyond 40dB
descended into the noise level of our pattern recorder.

Polarization and Feed Problems

Problems caused by a dipole feed are well known and are solved by using a horn feed. For this system the parasitic reflector helps to phase the rearward energy from the dipole and direct it onto the reflector. The resulting aperture distribution was not uniform without the movable discs on the reflector inner surface. The degree to which the non-uniform aperture distribution affected the phase-nulling of the discs was not investigated. The focal distance was varied, but had negligible effects on cancellation. Only the relative disc positions changed for a relative system null angle, for varied focal lengths.

A second shortcoming of the dipole feed is that some of the reflected energy is perpendicular to that of the primary radiation. The cross-polarized radiation causes the antenna gain to be reduced and side lobes with polarization orthogonal to the primary polarization are generated. This energy is wasted because the antenna might not be designed to respond to a different polarization.

Both effects can be minimized by a shallow reflector, one with a large ratio of focal length to diameter. The maximum theoretical aperture efficiency obtainable from a dipole-parasitic reflector feed is 69% (Skolnik, 1970:10-6). Theoretical aperture efficiencies obtainable for horn fed paraboloids are approximately 80% (Skolnik, 1962:273).

53

Effects Not Modeled

The repeatability of the measured patterns for the same disc positions proved to be a problem. It is not uncommon to produce a pattern at a specific null angle, then find the final disc positions to be off by as much as 0.5 cm from one pattern to the next. As another way to look at this, if one took the disc positions recorded in appendix D, set the discs according to the data, ran the patterns, the system nulls would come out slightly different each time (approximately $\pm$ 2°). This is due to a multitude of effects, the predominate one being the "quiet-zone" around the pedestal is not constant. Since the antenna system is mounted on top of the EM Technology Division's building at Hanscom AFB, the diffraction and reflection effects of the nearby equipment are constantly changing, as new and different equipment is set up. To get accurate patterns this system would have to be set up on a calibrated antenna range.

The thrust of this study was to investigate in a more simplified manner the phase nulling caused by the discs in the side lobes of the power pattern of the reflector. To more accurately model this phenomenom the diffraction pattern of the discs should be included in a geometrical theory of diffraction approach to overcome the simplified ray tracing approach used here. Other factors that should be more accurately modeled are: aperture blockage, errors in the paraboloid surface, and finally a horn fed antenna for uniform aperture illumination.

Summary and Recommendations

One of the basic problems with a movable disc system is the amount of time the computer takes to move the discs to their final position to minimize the total power of the received signal. Once the discs reach this final position a system null has been placed in the direction of the interferring source. It was not uncommon in the first systems to see 15 to 20 minutes go by, before disc optimum positons were established. Since then times of 5 minutes have been established by efficient computer programming techniques. It was hoped at the outset of the research that the physical optics approach might help alleviate this problem. It became apparent that the "speed" problem is beyond the scope of the thesis presented here. What the research does is provide a solid foundation upon which to build a geometrical theory of diffraction approach. With an accurate model in hand optimum disc position could be predicted rapidly. The research here did not address disc position or numbers of discs (more than two) on the reflector surface. This problem has already received a large amount of research time at the EM Technology Division at Hanscom AFB. Actual disc placement, size, and numbers of discs are more system specific. Developing unified guidelines for a generalized paraboloid would be difficult.

This study accomplished what it set out to do, investigating the phase nulling effects of the discs on the side lobe region of the far field radiation pattern. The next step would be to

generate field intensity amplitude and phase plots for a multitude of disc positions at one system null angle. The plots could be analyzed to find the optimum disc positions for equal amplitudes and opposite phases, then the power pattern generated, and compared to a measured power pattern using that optimum disc position. If the comparison was successful, then all optimum disc positions with their respective system null angles could be cataloged using this analysis. This would require quite a bit of time but would be valuable in addressing the "speed" problem of positioning the discs.

One might wonder how this system would be used ouside of the laboratory. An urban communication system which relies on reflectors exclusively would profit by using single fixed nulls to reduce specular reflections from large buildings. NASA which has plans for direct broadcast satellites could use this technique for receiving antennas on user's roofs to null out interference (Jacavanco, 1984a:2). In actual field tests at the EM Technology Division, Jacavanco has suppressed a high power mobile S-band source while maintaining a continuous link with a desired low power signal, fixed in position. Actually, the ultimate application will hopefully come in space to overcome the problems of the Electrostatic Membrane Reflector (page 1).

While this model is only a first order approximation it appears to accurately represent the two disc system. The linear array approach to model the reflector was used by Jacavanco (Jacavanco, 1984a), but the physical optics scattering off the

discs is unique. The model breaks down the nulling effect into two parts. The power contribution from the reflector and feed verses the power contribution from the discs. It is shown by proper disc placement that the amplitude of scattering off the discs can be made approximately equal to the amplitude in the side lobe region of the reflector and their phases close to 180° out of phase. A null in the far field power radiation pattern at a specific system null angle results. The mathematical model is implemented in Fortran 77-code. The theoretical patterns are compared to experimental patterns with a high degree of success.

V. Appendix

Appendix A. Variable Definitions and Values

1. f = 3.12 Ghz: antenna system frequency

2. λ = 9.62 cm: free space wavelength

3. $1 = \lambda/4$

4. $\beta = 2\pi/\lambda$

5. r = 5334 cm: 175 ft --> distance to transmitter from system phase reference. (the observation point)

6. q = 49.4 cm: see Appendix B

7. w = 36.9 cm: see Appendix B

8. θ_i = 26°: see Appendix B

9. r_o = 2.54 cm: radius of parasitic reflector

10. B = 20.3 cm^2: area of parasitic reflector

11. ρ_o = 6.35 cm: radius of movable disc

12. A = 126.7 cm^2: area of movable disc

13. f = 17.3 cm: antenna focal length (measured from dish vertex to parasitic reflector)

14. t_1 = distance of disc 1 from reflector face (flush = .3175 cm)

15. t_2 = distance of disc 2 from reflector face (flush = .3175 cm)

16. Radius of Dish = 32 cm

17. Aperture Plane Area = 3217 cm^2

18. E_o: normalized to 1.0

19. E_{os}: normalized to 0.0394 (figured as the ratio of the area of a disc to the area of dish aperture)

20. E_{ofb}: normalized to 0.0063 (figured as the ratio of the area of parasitic reflector to dish aperture area)

Figure 32. Scale Drawing for θ_i, w, q

59

Appendix C. Computer Program Fortran-77 Source Code

Program PHASENUL (page 62) calculates in one degree increments
$|\overline{E}_{TOT}(\theta,\phi=0)|^2$ for $-90° \leq \theta \leq +90°$. All programs were
compiled and executed using IBM PC-DOS 2.1 on a Corona Home
Computer. PHASENUL will execute upon typing the file name
PHASENUL at the system prompt. The data file CURRDIST.DAT must
reside on the same floppy disc as PHASENUL.EXE. CURRDIST.DAT
contains the array of normalized amplitudes of the isotropic
radiators which sample the aperture plane at quarter
wavelengths. The program asks for E_o, E_{os}, E_{ofb}, t_1,
t_2, (see Appendix A) on screen as input from the keyboard in
single precision accurracy. PHASENUL outputs a power point per
degree θ in a file called EPWRPT.DAT. The system quiescent
power pattern is generated by assigning:
$E_o = 1.0$, $E_{os} = 0.0394$, $E_{ofb} = 0.0063$, $t_1 = 0.3175$,
$t_2 = 0.3175$. All other power patterns are generated by
leaving E_o, E_{os}, E_{ofb} fixed at 1.0, 0.0394, 0.0063
respectively and assigning t_1 and t_2 from Appendix D. The
bessel function in all programs is approximated by its series
expansion to the third term.

Program PHASCANL (page 68) calculates in one degree increments
$|\overline{E}_C(\theta,\phi=0)|$ for $-90° \leq \theta \leq +90°$.
PHASCANL will execute upon typing the filename PHASCANL at the
system prompt. The program asks for E_{os}, t_1, t_2 (see

60

Appendix A) on screen as input from the keyboard in single

precision accurracy. PHASCANL outputs a phase point and

amplitude point per degree θ in files called PHASEC.DAT and

AMPL.DAT respectively. The plots were generated by leaving

E_{os} = 0.0394 and assigning t_1 and t_2 from Appendix D.

Program PHASEQ (page 71) calculates in one degree

increments $|\bar{E}_Q(\theta,\phi=0)|$ for $-90° \leq \theta \leq +90°$. PHASEQ will

execute upon typing the filename PHASEQ at the system prompt.

The program asks for E_o, E_{os}, E_{ofb}, t_1, t_2 (see

Appendix A) on screen as input from the keyboard in single

precision accuracy. PHASEQ outputs a phase point and amplitude

point per degree θ in files called PHASEQ.DAT and AMPL.DAT

respectively. The plots were generated by leaving E_o = 1.0,

E_{os} = 0, E_{ofb} =0.0063, t_1 = 0.3175, and t_2 = 0.3175.

This generates the quiescent plots without discs.

All graphs were generated by using Lotus 123 (Lotus

Development Corporation, Cambridge, Massachusetts)

```
          PROGRAM PHASENUL
*
*
*
*
*    Input variables (real):
*          Q:
*          L:
*          K:
*          LAMBDA:
*          F:
*          BETAX:
*          BETAY:
*          BETAZ:
*          THETA:
*          R:
*          E0:
*          IXY:
*
*    Output variables:
*          EXY:
*
*
*
          INTEGER A,B,C,D,E,F,DEG(181),THETADEG,M
*
          REAL Q,L,K,LAMBDA,FREQ,BETAX,BETAZ,THETA,R,E0,SINTH,COSPLTHI
          REAL IXY(29,29),PI,BESSEL,X1,COSTH,COSMITHI,BESARG1,SINTHI
          REAL BESARG2,T1ARG,T2ARG,SINT1ARG,SINT2ARG,ESCONST,COSTHI
          REAL THETAI,AREA,RO,T1,T2,W,B1,R0,U,ENORM,EPWRPT
          REAL BESFNT1,BESFNT2,BESFNCT,AMAG(181),AMAGATO
*
*
          COMPLEX EXY(29,29),COLTOTAL,ROWTOTAL,EFIELD(29),S,S1
          COMPLEX ENDTH(181),EBETAZ,JCMPLX,MJCMPLX,EFBTH(181),ETOTAL
          COMPLEX ES12TH(181),EJKW,EJKR,EJKT1,EJKT2,EFBCONST,EXJKQCOS
*
*
*    Open input and output files
*
          OPEN (2,FILE='CURRDIST.DAT',STATUS='UNKNOWN')
          OPEN (3,FILE='END.DAT',STATUS='UNKNOWN')
          OPEN (9,FILE='ES12TH.DAT',STATUS='UNKNOWN')
          OPEN (10,FILE='EFBTH.DAT',STATUS='UNKNOWN')
          OPEN (11,FILE='AMAG.DAT',STATUS='UNKNOWN')
*
*
*    Initialize arrays
*
          DO 55 I=1,29
               DO 50 J=1,29
                    EXY(I,J)=(0.0,0.0)
                    IXY(I,J)=0.0
50             CONTINUE
55        CONTINUE
*
```

62

```
              DO 60 I=1,29
                  COLTOTAL=(0.0,0.0)
                  ROWTOTAL=(0.0,0.0)
60        CONTINUE
*
*
*   Read current amplitude distribution factors
*
          DO 100 I=1, 29
              READ (2,*,END=1000) (IXY(I,J), J=1, 29)
              WRITE(*,*) (IXY(I,J),J=1,29)
100       CONTINUE
*
          CLOSE (2)
*
*   Initialize constant parameters
*
          Q=49.4
          L=2.41
          LAMBDA=9.62
          PI=3.1415926
          K=2*PI/LAMBDA
          JCMPLX=CMPLX(0.0,1.0)
          MJCMPLX=CMPLX(0.0,-1.0)
          R=5334.0
*
*
*   Input initial E-field amplitude distribution, E0
*
          WRITE(*,*)
          WRITE(*,'(A)')' ENTER VALUE FOR E0'
          WRITE(*,*)
          READ *, E0
          WRITE (*,120) E0
120       FORMAT('0','E0 =  ',F6.4)
*
*
*   Compute exponential factors for all rows and thetas
*
          DO 500 I=1, 181
              THETADEG=I-91
*             WRITE(*,112) THETADEG
*112           FORMAT(' ',' THETA = ',I4, ' DEGREES')
              THETA= (I-91)*PI/180
              BETAX=-K*SIN(THETA)
              BETAZ=-K*COS(THETA)
              ERETAZ=CEXP(CMPLX(0.0,-BETAZ*Q))
*
              DO 300 A=1,29
                  DO 200 B=1,29
                      M=15-B
                      EXY(A,B)=CEXP(CMPLX(0.0,-BETAX*M*L))
                      COLTOTAL=COLTOTAL+IXY(A,B)*EXY(A,B)
200               CONTINUE
              ROWTOTAL=ROWTOTAL+COLTOTAL
```

```fortran
                COLTOTAL=(0.0,0.0)
300             CONTINUE
*

                S=CEXP(CMPLX(0.0,-K*R))
                S1=JCMPLX*E0*K*S/(2*PI*R)
                ENDTH(I)=S1*EBETAZ*ROWTOTAL
                WRITE(3,*) THETADEG, ENDTH(I)
*

                ROWTOTAL=(0.0,0.0)
500     CONTINUE
122     FORMAT (' ',' FOR THETA = ',I4,' E-FIELD = ',2F12.5)
*

*

*       DO 125, I=1, 181
*            READ(3,*,END=125) DEG(I),EFIELD(I)
*            WRITE(*,*) DEG(I), EFIELD(I)
125     CONTINUE
*

*       E-FIELD OF DISKS 1 AND 2
*

*   Input initial E-field amplitude distribution, E0S
*
510     WRITE(*,*)
        WRITE(*,'(A)')' ENTER VALUE FOR E0S'
        WRITE(*,*)
        READ *, E0S
        WRITE (*,520) E0S
520     FORMAT('0','E0S =  ',F12.9)
*

*

*   Input phase distance, T1
*
530     WRITE(*,*)
        WRITE(*,'(A)')' ENTER VALUE FOR T1'
        WRITE(*,*)
        READ *, T1
        WRITE (*,540) T1
540     FORMAT('0','T1 =  ',F6.4)
*

*   Input phase distance, T2
*
550     WRITE(*,*)
        WRITE(*,'(A)')' ENTER VALUE FOR T2'
        WRITE(*,*)
        READ *, T2
        WRITE (*,560) T2
560     FORMAT('0','T2 =  ',F6.4)
*
580     RO=6.35
        W=36.9
        THETAI=26*PI/180
        COSTHI=COS(THETAI)
        SINTHI=SIN(THETAI)
        AREA=126.7
        EJKR=CEXP(CMPLX(0.0,-K*R))
```

```
            ESCONST=(E0S*K)/(PI*R)
*
            DO 600 I=1, 181
                THETADEG=I-91
                THETA=THETADEG*PI/180
                COSTH=COS(THETA)
                SINTH=SIN(THETA)
                COSPLTHI=COS(THETAI+THETA)
                COSMITHI=COS(THETAI-THETA)
                BESARG1=K*RO*(SINTH+SINTHI)
                BESARG2=K*RO*(SINTH-SINTHI)
                EJKW=CEXP(CMPLX(0.0,K*W*COSTH))
                T1ARG=(K*T1/2)*(COSTHI+COSPLTHI)
                T2ARG=(K*T2/2)*(COSTHI+COSMITHI)
                EJKT1=CEXP(CMPLX(0.0,T1ARG))
                EJKT2=CEXP(CMPLX(0.0,T2ARG))
                SINT1ARG=SIN(T1ARG)
                SINT2ARG=SIN(T2ARG)
*
                IF(THETADEG.EQ. -26) THEN
                    BESFNT1 = .5
                ELSE
                    BESFNT1 = BESSEL(BESARG1)/BESARG1
                END IF
*
*
                IF (THETADEG .EQ. 26) THEN
                    BESFNT2 = .5
                ELSE
                    BESFNT2 = BESSEL(BESARG2)/BESARG2
                END IF
*
                ES12TH(I)=-(ESCONST*EJKR*EJKW*COSTHI*AREA*((2*BESFNT1
     +                  *SINT1ARG*EJKT1)+(2*BESFNT2
     +                  *SINT2ARG*EJKT2)))
                WRITE(9,*) THETADEG, ES12TH(I)
                WRITE(*,601) THETADEG, ES12TH(I)
*601            FORMAT(' ','THETA = ',I4,' E-FIELD OF DISKS 1&2 = ',2F10.8)
*
600         CONTINUE
*
*
*           E-FIELD OF FEED
*
*   Input initial E-field amplitude distribution, E0FB
*
650         WRITE(*,*)
            WRITE(*,'(A)')' ENTER VALUE FOR E0FB'
            WRITE(*,*)
            READ *, E0FB
            WRITE (*,660) E0FB
660         FORMAT('0','E0FB =  ',F8.6)
*
680         B1=20.3
            RO=2.54
```

65

```
*
            DO 700 I=1, 181
                THETADEG=I-91
                THETA=THETADEG*PI/180
                SINTH=SIN(THETA)
                COSTH=COS(THETA)
                EFBCONST=CMPLX(0.0,(E0FB*K)/(2*PI*R))
                EXJKOCOS=CEXP(CMPLX(0.0,K*O*COSTH))
                U=K*R0*SINTH
*
                IF (THETADEG .EQ. 0) THEN
                    BESFNCT = .5
                ELSE
                    BESFNCT = BESSEL(U)/U
                END IF
*
                EFBTH(I)=EFBCONST*EJKR*EXJKOCOS*B1*2*(BESFNCT)
701             WRITE(10,*) THETADEG, EFBTH(I)
*               WRITE(*,701) THETADEG, EFBTH(I)
*702            FORMAT(' ','THETA = ',I4,' E-FIELD OF FEED = ',2F10.8)
*
700         CONTINUE
*
            OPEN (13,FILE='ETOTAL.DAT',STATUS='UNKNOWN')
*
*   TOTAL E-FIELDS
*
*
780         DO 800 I=1, 181
                THETADEG=I-91
                ETOTAL=ENDTH(I)-ES12TH(I)-EFBTH(I)
*
                WRITE(13,*) THETADEG, ETOTAL
*               WRITE(*,781) THETADEG, ETOTAL
*781            FORMAT(' ','THETA = ',I4,' E-FIELD TOTAL = ',2F12.8)
*
                AMAG(I)=REAL(ETOTAL)**2+AIMAG(ETOTAL)**2
*
                IF (THETADEG .EQ. 0) THEN
                    AMAGAT0=AMAG(I)
                END IF
*
                WRITE(11,*) THETADEG, AMAG(I)
*               WRITE(*,801) THETADEG, AMAG(I)
*801            FORMAT(' ','THETA = ',I4,' MAGNITUDE OF E-FIELD = ',F12.5)
*
800         CONTINUE
            CLOSE (13)
*
            OPEN (12,FILE='EPWRPT.DAT',STATUS='UNKNOWN')
*
            DO 900 I=1, 181
                THETADEG=I-91
                ENORM=AMAG(I)/AMAGAT0
                EPWRPT=10*ALOG10(ENORM)
```

```
              WRITE(12,*) THETADEG, EPWRPT
              WRITE(*,901) THETADEG, EPWRPT
*901          FORMAT(' ','THETA = ',I4,' POWER PTS OF E-FIELD = ',F10.8)
900     CONTINUE
*
1000    END
*
*  BESSEL FUNCTION ROUTINE
*
        REAL FUNCTION BESSEL(X1)
        REAL X1,BES1
*
        BES1=(X1/2)-(X1**3)/(2**3*2)+(X1**5)/(2**5*12)
        BESSEL=BES1
*
        RETURN
        END
```

```
          PROGRAM  PHASCANL
*
          INTEGER A,B,C,D,E,F,DEG(181),THETADEG
*
          REAL K,LAMBDA,THETA,R,EOS,SINTH,COSPLTHI
          REAL PI,BESSEL,X1,COSTH,COSMITHI,BESARG1,SINTHI
          REAL BESARG2,T1ARG,T2ARG,SINT1ARG,SINT2ARG,ESCONST,COSTHI
          REAL THETAI,AREA,RO,T1,T2,W,R0,PHASE
          REAL BESFNT1,BESFNT2,BESFNCT,AMPL(181),PHASEC(181)
*
*
          COMPLEX ETOTÅL
          COMPLEX ES12TH(181),EJKW,EJKR,EJKT1,EJKT2
*
*
*   Open input and output files
*
          OPEN (9,FILE='ES12TH.DAT',STATUS='UNKNOWN')
*
*
*
*         E-FIELD OF DISKS 1 AND 2
*
*   Input initial E-field amplitude distribution, EOS
*
510       WRITE(*,*)
          WRITE(*,'(A)')' ENTER VALUE FOR EOS'
          WRITE(*,*)
          READ *, EOS
          WRITE (*,520) EOS
520       FORMAT('0','EOS =  ',F12.9)
*
*
*   Input phase distance, T1
*
530       WRITE(*,*)
          WRITE(*,'(A)')' ENTER VALUE FOR T1'
          WRITE(*,*)
          READ *, T1
          WRITE (*,540) T1
540       FORMAT('0','T1 =  ',F6.4)
*
*   Input phase distance, T2
*
550       WRITE(*,*)
          WRITE(*,'(A)')' ENTER VALUE FOR T2'
          WRITE(*,*)
          READ *, T2
          WRITE (*,560) T2
560       FORMAT('0','T2 =  ',F6.4)
*
580       RO=6.35
          W=36.9
          PI=3.1415926
          THETAI=26*PI/180
```

```fortran
         COSTHI=COS(THETAI)
         SINTHI=SIN(THETAI)
         AREA=126.7
         LAMBDA=9.62
         R=5334.0
         K=2*PI/LAMBDA
         EJKR=CEXP(CMPLX(0.0,-K*R))
         ESCONST=(E0S*K)/(PI*R)
         AMAGATO=.000005696
*
         ESCONST=(E0S*K)/(PI*R)
*
         DO 600 I=1, 181
              THETADEG=I-91
              THETA=THETADEG*PI/180
              COSTH=COS(THETA)
              SINTH=SIN(THETA)
              COSPLTHI=COS(THETAI+THETA)
              COSMITHI=COS(THETAI-THETA)
              BESARG1=K*RO*(SINTH+SINTHI)
              BESARG2=K*RO*(SINTH-SINTHI)
              EJKW=CEXP(CMPLX(0.0,K*W*COSTH))
              T1ARG=(K*T1/2)*(COSTHI+COSPLTHI)
              T2ARG=(K*T2/2)*(COSTHI+COSMITHI)
              EJKT1=CEXP(CMPLX(0.0,T1ARG))
              EJKT2=CEXP(CMPLX(0.0,T2ARG))
              SINT1ARG=SIN(T1ARG)
              SINT2ARG=SIN(T2ARG)
*
              IF(THETADEG.EQ. -26) THEN
                  BESFNT1 = .5
              ELSE
                  BESFNT1 = BESSEL(BESARG1)/BESARG1
              END IF
*
*
              IF (THETADEG .EQ. 26) THEN
                   BESFNT2 = .5
              ELSE
                   BESFNT2 = BESSEL(BESARG2)/BESARG2
              END IF
*
              ES12TH(I)=(ESCONST*EJKR*EJKW*COSTHI*AREA*((2*BESFNT1
     +               *SINT1ARG*EJKT1)+(2*BESFNT2
     +               *SINT2ARG*EJKT2)))
              WRITE(9,*) THETADEG, ES12TH(I)
*              WRITE(*,601) THETADEG, ES12TH(I)
*601          FORMAT(' ','THETA = ',I4,' E-FIELD OF DISKS 1&2 = ',2F10.8)
*
600      CONTINUE
*
*
*
         OPEN (13,FILE='AMPL.DAT',STATUS='UNKNOWN')
         OPEN (14,FILE='PHASEC.DAT',STATUS='UNKNOWN')
```

```
*
*   TOTAL E-FIELDS
*
,60         DO 700 I=1, 181
                THETADEG=I-91
                ETOTAL=ES12TH(I)
                PHASE=ATAN(AIMAG(ETOTAL)/REAL(ETOTAL))
                PHASEC(I)=(PHASE*360)/(2*PI)
                WRITE(14,*) THETADEG, PHASEC(I)
700         CONTINUE
*
780         DO 800 I=1, 181
                THETADEG=I-91
                ETOTAL=ES12TH(I)
                AMPL(I)=(REAL(ETOTAL)**2+AIMAG(ETOTAL)**2)**.5
                WRITE(13,*) THETADEG, AMPL(I)
800         CONTINUE
*
1000        END
*
*  BESSEL FUNCTION ROUTINE
*
            REAL FUNCTION BESSEL(X1)
            REAL X1,BES1
*
            BES1=(X1/2)-(X1**3)/(2**3*2)+(X1**5)/(2**5*12)
            BESSEL=BES1
*
            RETURN
            END
```

```
        PROGRAM PHASEQ
*
        INTEGER A,B,C,D,E,F,DEG(181),THETADEG,M
*
        REAL D,L,K,LAMBDA,FREQ,BETAX,BETAZ,THETA,R,EQ,SINTH,COSPLTHI
        REAL IXY(29,29),PI,BESSEL,X1,COSTH,COSMITHI,BESARG1,SINTHI
        REAL BESARG2,T1ARG,T2ARG,SINT1ARG,SINT2ARG,ESCONST,COSTHI
        REAL THETAI,AREA,RO,T1,T2,W,B1,RO,U,PHASEQ(181)
        REAL BESFNT1,BESFNT2,BESFNCT,AMPL(181),PHASE
*
*

        COMPLEX EXY(29,29),COLTOTAL,ROWTOTAL,EFIELD(29),S,S1
        COMPLEX ENDTH(181),EBETAZ,JCMPLX,MJCMPLX,EFBTH(181),ETOTAL
        COMPLEX ES12TH(181),EJKW,EJKR,EJKT1,EJKT2,EFBCONST,EXJKQCOS
*
*
*  Open input and output files
*
        OPEN (2,FILE='CURRDIST.DAT',STATUS='UNKNOWN')
        OPEN (3,FILE='END.DAT',STATUS='UNKNOWN')
        OPEN (9,FILE='ES12TH.DAT',STATUS='UNKNOWN')
        OPEN (10,FILE='EFBTH.DAT',STATUS='UNKNOWN')
*
*
*  Initialize arrays
*
        DO 55 I=1,29
            DO 50 J=1,29
                EXY(I,J)=(0.0,0.0)
                IXY(I,J)=0.0
50          CONTINUE
55      CONTINUE
*
        DO 60 I=1,29
            COLTOTAL=(0.0,0.0)
            ROWTOTAL=(0.0,0.0)
60      CONTINUE
*
*
*  Read current amplitude distribution factors
*
        DO 100 I=1, 29
            READ (2,*,END=1000) (IXY(I,J), J=1, 29)
            WRITE(*,*) (IXY(I,J),J=1,29)
100     CONTINUE
*
        CLOSE (2)
*
*  Initialize constant parameters
*
        D=49.4
        L=2.41
        LAMBDA=9.62
        PI=3.1415926
        K=2*PI/LAMBDA
```

71

```
          JCMPLX=CMPLX(0.0,1.0)
          MJCMPLX=CMPLX(0.0,-1.0)
          R=5334.0
*
*
*   Input initial E-field amplitude distribution, E0
*
          WRITE(*,*)
          WRITE(*,'(A)')' ENTER VALUE FOR E0'
          WRITE(*,*)
          READ *, E0
          WRITE (*,120) E0
120       FORMAT('0','E0 =   ',F6.4)
*
*                                 .
*   Compute exponential factors for all rows and thetas
*
          DO 500 I=1, 181
               THETADEG=I-91
*              WRITE(*,112) THETADEG
#112           FORMAT(' ',' THETA = ',I4, ' DEGREES')
               THETA= (I-91)*PI/180
               BETAX=-K*SIN(THETA)
               BETAZ=-K*COS(THETA)
               EBETAZ=CEXP(CMPLX(0.0,-BETAZ*D))
*
               DO 300 A=1,29
                    DO 200 B=1,29
                         M=15-B
                         EXY(A,B)=CEXP(CMPLX(0.0,-BETAX*M*L))
                         COLTOTAL=COLTOTAL+IXY(A,B)*EXY(A,B)
200                 CONTINUE
               ROWTOTAL=ROWTOTAL+COLTOTAL
               COLTOTAL=(0.0,0.0)
300            CONTINUE
*
               S=CEXP(CMPLX(0.0,-K*R))
               S1=JCMPLX*E0*K*S/(2*PI*R)
               ENDTH(I)=S1*EBETAZ*ROWTOTAL
               WRITE(3,*) THETADEG, ENDTH(I)
*
               ROWTOTAL=(0.0,0.0)
500       CONTINUE
122       FORMAT (' ',' FOR THETA = ',I4,' E-FIELD = ',2F12.5)
*
*
*         DO 125, I=1, 181
*              READ(3,*,END=125) DEG(I),EFIELD(I)
*              WRITE(*,*) DEG(I), EFIELD(I)
125       CONTINUE
*
*         E-FIELD OF DISKS 1 AND 2
*
*   Input initial E-field amplitude distribution, E0S
*
```

```
510       WRITE(*,*)
          WRITE(*,'(A)')' ENTER VALUE FOR EOS'
          WRITE(*,*)
          READ *, EOS
          WRITE (*,520) EOS
520       FORMAT('0','EOS = ',F12.9)
*
*
*   Input phase distance, T1
*
530       WRITE(*,*)
          WRITE(*,'(A)')' ENTER VALUE FOR T1'
          WRITE(*,*)
          READ *, T1
          WRITE (*,540) T1
540       FORMAT('0','T1 = ',F6.4)
*
*   Input phase distance, T2
*
550       WRITE(*,*)
          WRITE(*,'(A)')' ENTER VALUE FOR T2'
          WRITE(*,*)
          READ *, T2
          WRITE (*,560) T2
560       FORMAT('0','T2 = ',F6.4)
*
580       RO=6.35
          W=36.9
          THETAI=26*PI/180
          COSTHI=COS(THETAI)
          SINTHI=SIN(THETAI)
          AREA=126.7
          EJKR=CEXP(CMPLX(0.0,-K*R))
          ESCONST=(EOS*K)/(PI*R)
*
          DO 600 I=1, 181
              THETADEG=I-91
              THETA=THETADEG*PI/180
              COSTH=COS(THETA)
              SINTH=SIN(THETA)
              COSPLTHI=COS(THETAI+THETA)
              COSMITHI=COS(THETAI-THETA)
              BESARG1=K*RO*(SINTH+SINTHI)
              BESARG2=K*RO*(SINTH-SINTHI)
              EJKW=CEXP(CMPLX(0.0,K*W*COSTH))
              T1ARG=(K*T1/2)*(COSTHI+COSPLTHI)
              T2ARG=(K*T2/2)*(COSTHI+COSMITHI)
              EJKT1=CEXP(CMPLX(0.0,T1ARG))
              EJKT2=CEXP(CMPLX(0.0,T2ARG))
              SINT1ARG=SIN(T1ARG)
              SINT2ARG=SIN(T2ARG)
*
              IF(THETADEG.EQ. -26) THEN
                  BESFNT1 = .5
              ELSE
```

73

```
                    BESFNT1 = BESSEL(BESARG1)/BESARG1
                END IF
*
*

                IF (THETADEG .EQ. 26) THEN
                    BESFNT2 = .5
                ELSE
                    BESFNT2 = BESSEL(BESARG2)/BESARG2
                END IF
*
                ES12TH(I)=-(ESCONST*EJKR*EJKW*COSTHI*AREA*((2*BESFNT1
       +                *SINT1ARG*EJKT1)+(2*BESFNT2
       +                *SINT2ARG*EJKT2)))
                WRITE(9,*) THETADEG, ES12TH(I)
                WRITE(*,601) THETADEG, ES12TH(I)
*601            FORMAT(' ','THETA = ',I4,' E-FIELD OF DISKS 1&2 = ',2F10.8)
*
600     CONTINUE
*
*
*       E-FIELD OF FEED
*
*   Input initial E-field amplitude distribution, E0FB
*
650     WRITE(*,*)
        WRITE(*,'(A)')' ENTER VALUE FOR E0FB'
        WRITE(*,*)
        READ *, E0FB
        WRITE (*,660) E0FB
660     FORMAT('0','E0FB = ',F8.6)
*
680     B1=20.3
        R0=2.54
*
        DO 700 I=1, 181
            THETADEG=I-91
            THETA=THETADEG*PI/180
            SINTH=SIN(THETA)
            COSTH=COS(THETA)
            EFBCONST=CMPLX(0.0,(E0FB*K)/(2*PI*R))
            EXJKQCOS=CEXP(CMPLX(0.0,K*Q*COSTH))
            U=K*R0*SINTH
*
            IF (THETADEG .EQ. 0) THEN
                BESFNCT = .5
            ELSE
                BESFNCT = BESSEL(U)/U
            END IF
*
            EFBTH(I)=EFBCONST*EJKR*EXJKQCOS*B1*2*(BESFNCT)
701         WRITE(10,*) THETADEG, EFBTH(I)
*           WRITE(*,701) THETADEG, EFBTH(I)
*702        FORMAT(' ','THETA = ',I4,' E-FIELD OF FEED = ',2F10.6)
*
700     CONTINUE
```

74

```
*
          OPEN (13,FILE='AMPL.DAT',STATUS='UNKNOWN')
          OPEN (14,FILE='PHASEQ.DAT',STATUS='UNKNOWN')
*
*    TOTAL E-FIELDS
*
760       DO 750 I=1, 181
              THETADEG=I-91
              ETOTAL=ENDTH(I)-ES12TH(I)-EFBTH(I)
              PHASE=ATAN(AIMAG(ETOTAL)/REAL(ETOTAL))
              PHASEQ(I)=(PHASE*360)/(2*PI)
              WRITE(14,*) THETADEG, PHASEQ(I)
750       CONTINUE
*
780       DO 800 I=1, 181
              THETADEG=I-91
              ETOTAL=ENDTH(I)-ES12TH(I)-EFBTH(I)
              AMPL(I)=(REAL(ETOTAL)**2+AIMAG(ETOTAL)**2)**.5
              WRITE(13,*) THETADEG, AMPL(I)
800       CONTINUE
*
1000      END
*
*   BESSEL FUNCTION ROUTINE
*
          REAL FUNCTION BESSEL(X1)
          REAL X1,BES1
*
          BES1=(X1/2)-(X1**3)/(2**3*2)+(X1**5)/(2**5*12)
          BESSEL=BES1
*
          RETURN
          END
```

Appendix D. Measured Data

Measured Data

PATTERN	Disc 1	Disc2
Figure 18, 19 System Null at: $\theta = +35^\circ$	$t_1 = 5.4$ cm	$t_2 = 4.6$ cm
Figure 20, 21 System Null at: $\theta = -20^\circ,\ +20^\circ$	$t_1 = 5.4$ cm	$t_2 = 5.2$ cm
Figure 22, 23 System Null at: $\theta = -35^\circ$	$t_1 = 4.9$ cm	$t_2 = 5.2$ cm
Figure 24, 25 System Null at: $\theta = -45^\circ$	$t_1 = $ Flush (.3175 cm)	$t_2 = 6.3$ cm
Figure 26, 27 System Null at: $\theta = -60^\circ$	$t_1 = 7.6$ cm	$t_2 = $ Full Extension (8.7 cm)

Bibliography

Havens, Douglas A. _Pattern Nulling by Reflector Shaping_. MS Thesis 83D-26. School of Engineering, Air Force Institute of Technology (AU), Wright-Patterson AFB OH. December 1983.

Jacavanco, Daniel. "Controlled Surface Distortion Effects," _Proceedings of the 1984 Antenna Applications Symposium_. Robert Allerton Park, University of Illinois, 1984a.

Jacavanco, Daniel. "Nulling in a Reflector Antenna by Dynamic Surface Control," RADC-TR-85-125, 1984b.

-----. "Adaptive Reflectors." Current work briefing to AFIT personnel. Rome Air Development Center, Hanscom AFB MA, 20 March 1984c.

-----. Interview and research notes form Prof. R. Rudduck. Electrical Engineering Department, Ohio State University, Columbus, Ohio, 18 June 1985a.

-----. Interviews and research notes from Dr. J. Leon Poirier. Electromagnetic Technology Applications Section, Rome Air Development Center, Hanscom AFB MA, 3-7 June 1985b.

-----. Interviews with Daniel Jacavanco. Electromagnetic Technology Applications Section, Rome Air Development Center, Hanscom AFB MA, 3-7 June 1985c.

Johnson, T. W. _Physical Optics Calculation of Radar Cross Section of Flat Metal Plate_. Instructor Notes. School of Engineering, Air Force Institute of Technology (AU). Wright-Patterson AFB OH, 1984.

Lang, J. H. and David H. Staelin. "Electrostatically-Controlled Large-Aperture Reflecting Satellite Antennas," _Proceedings of the IEEE Conference on Decision and Control_, 1980: 750-754.

Ling, Hao and Shung-Wu Lee, Peter T. C. Lam, and Willard V. T. Rusch. "Focal Shifts in Parabolic Reflectors," _IEEE Transactions on Antennas and Propagation_, AP-33: 744-748 (July 1985).

Ruck, George T., Donald E. Barrick, William D. Stuart, and Clarence K. Krichbaum. _Radar Cross Section Handbook_. Vol 2. New York-London: Plenum Press, 1970.

Rudisill, Michael D. *Null Generation Using Discs on a Reflector*. MS Thesis 84D-55. School of Engineering, Air Force Institute of Technology (AU), Wright-Patterson AFB OH, December 1984a.

Rudisill, Michael D. "Null Generation by Phase Perturbations in a Aperture," *Proceedings of the 1984 Antenna Applications Symposium*. Robert Allerton Park, University of Illinois, 1984b.

Skolnik, Merrill I. *Introduction to Radar Systems*. New York: McGraw-Hill Book Co. Inc., 1962.

Skolnik, Merrill I. *Radar Handbook*. New York: McGraw-Hill Book Co. Inc., 1970.

Stutzman, Warren L. and Gary A. Thiele. *Antenna Theory and Design*. New York: John Wiley and Sons, Inc., 1981.
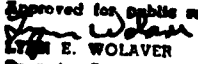
<u>Vita</u>

Captain Dick A. Trapp was born on 14 November 1953 in Montgomery, Alabama. During June 1972 he graduated from Brookings High School, South Dakota, and that fall attended South Dakota State University (SDSU) also in Brookings. He received the degree of Bachelor of Science in Electrical Engineering in December 1976 from SDSU. His commission in the USAF was obtained through the Air Force Reserve Officer Training Program while attending SDSU. He earned his pilot wings through Vance AFB, Enid, Oklahoma, graduating on 30 November 1978. He then served as an EC-135 pilot at Ellsworth AFB in the 4th Airborne Command and Control Squadron until March 1982. After completion of a tour as an Aircraft Commander, KC-135, at Dyess AFB in the 917th Air Refueling Squadron in May 1984, he was assigned to the School of Engineering, Air Force Institute of Technology.

Permanent Address: RR1 Box 150A
Volga, S.D. 57071

AD-A163 856

SECURITY CLASSIFICATION OF THIS PAGE

REPORT DOCUMENTATION PAGE

1a. REPORT SECURITY CLASSIFICATION UNCLASSIFIED	1b. RESTRICTIVE MARKINGS
2a. SECURITY CLASSIFICATION AUTHORITY	3. DISTRIBUTION/AVAILABILITY OF REPORT
2b. DECLASSIFICATION/DOWNGRADING SCHEDULE	Approved for public release; distribution unlimited

4. PERFORMING ORGANIZATION REPORT NUMBER(S) AFIT/GE/ENG/85D-51	5. MONITORING ORGANIZATION REPORT NUMBER(S)

6a. NAME OF PERFORMING ORGANIZATION School of Engineering	6b. OFFICE SYMBOL (If applicable) AFIT/ENG	7a. NAME OF MONITORING ORGANIZATION

6c. ADDRESS (City, State and ZIP Code) Air Force Institute of Technology Wright-patterson AFB, Ohio 45433	7b. ADDRESS (City, State and ZIP Code)

8a. NAME OF FUNDING/SPONSORING ORGANIZATION ELectromagnetic Sciences Div	8b. OFFICE SYMBOL (If applicable) RADC/EEC	9. PROCUREMENT INSTRUMENT IDENTIFICATION NUMBER

8c. ADDRESS (City, State and ZIP Code) Em Technology Applications Hanscom AFB, MA 01731	10. SOURCE OF FUNDING NOS.			
	PROGRAM ELEMENT NO.	PROJECT NO.	TASK NO	WORK UNIT NO

11. TITLE (Include Security Classification)
See Box 19

12. PERSONAL AUTHOR(S)
Dick A. Trapp, B.S., Capt, USAF

13a. TYPE OF REPORT MS Thesis	13b. TIME COVERED FROM _____ TO _____	14. DATE OF REPORT (Yr., Mo., Day) 1985 December	15. PAGE COUNT 79

16. SUPPLEMENTARY NOTATION

17	COSATI CODES		18. SUBJECT TERMS (Continue on reverse if necessary and identify by block number)
FIELD	GROUP	SUB. GR	Antenna Radiation Patterns, Antenna Side Lobes,
17	04		Adaptive Communications, Electronic Antijamming

19. ABSTRACT (Continue on reverse if necessary and identify by block number)

Title: PHYSICAL OPTICS MODEL OF
SIDE LOBE NULLING BY DISCS
ON A PARABOLIC REFLECTOR

Thesis Chairman: Dr. Andrew J. Terzuoli
Assistant Professor of Electrical Engineering

Approved for public release: IAW AFR 190-1.
LYNN E. WOLAVER   16 JAN 86
Dean for Research and Professional Development
Air Force Institute of Technology (ATC)
Wright-Patterson AFB OH 45433

20. DISTRIBUTION/AVAILABILITY OF ABSTRACT	21. ABSTRACT SECURITY CLASSIFICATION
UNCLASSIFIED/UNLIMITED ☒ SAME AS RPT ☐ DTIC USERS ☐	UNCLASSIFIED

22a. NAME OF RESPONSIBLE INDIVIDUAL Dr. Andrew J. Terzuoli	22b. TELEPHONE NUMBER (Include Area Code) 513-255-6913	22c. OFFICE SYMBOL AFIT/ENG

DD FORM 1473, 83 APR   EDITION OF 1 JAN 73 IS OBSOLETE.

SECURITY CLASSIFICATION OF THIS PAGE

Abstract

By mounting small disc reflectors that are moveable relative
to the inner reflector surface of a parabolic dish antenna,
nulls can be generated in the side lobe region of the power
radiation pattern with minimal distortion effects to the main
beam. A physical optics model of this antenna system is
developed to investigate in a simplified direct manner the
phenomena of phase nulling caused by disc movement.

Array theory using isotropic radiators is used to sample the
aperture distribution to approximate the far field electric
field of the dish. A physical optics approximation for
scattering off a flat metal disc is used for discs and feed
blockage effects. The array theory term plus the feed blockage
term yields the field intensity quiescent patterns, phase and
amplitude, proportional to $|\overline{E}_{Quiescent}(\Theta,\phi)|$. The physical
optics term for the discs yields the field intensity
cancellation patterns, phase and amplitude, proportional to
$|\overline{E}_{Cancellation}(\Theta,\phi)|$. The quiescent patterns are combined
with the cancellation patterns to produce the relative power
pattern, nulled pattern, proportional to $|\overline{E}_{Total}(\Theta,\phi)|^2$.
No secondary effects such as diffraction or edge
illumination are considered.

A computer code was written to implement this
approach and the theoretical patterns produced.
Actual measured patterns are compared to the
theoretical patterns. There is good agreement
between theory and actual measurements. Finally
applications of this antenna system are presented.

END

FILMED

3-86

DTIC